

# Experimental Analysis of Smart Tires

by

Hasan Toplar

A thesis  
presented to the University of Waterloo  
in fulfillment of the  
thesis requirement for the degree of  
Master of Applied Science  
in  
Mechanical Engineering

Waterloo, Ontario, Canada, 2014

© Hasan Toplar 2014

## **AUTHOR'S DECLARATION**

I hereby declare that I am the sole author of this thesis. This is a true copy of the thesis, including any required final revisions, as accepted by my examiners.

I understand that my thesis may be made electronically available to the public.

## Abstract

A novel smart tire monitoring system was designed and implemented on a fully functional car tire. Polyvinylidene fluoride (PVDF) based piezo-electric sensors were embedded inside rubber tire to measure strain related data. System electronics were implemented inside a robust IP-68 (Ingress Protection) rated enclosure. This enclosure was mounted on a car wheel and successfully recorded sensory data onto an SD card during driving. Data collected from the PVDF sensors were then post-processed in Matlab. An artificial neural network (ANN) was built to correlate the sensor data to the readings given by an industry grade load wheel. Although the correlations are very crude, this study shows a promising way to analyze the strain related information from car tires by using PVDF sensors in conjunction with ANNs. This strain related information can then be used to estimate six different values concerning the tire, namely lateral force ( $F_y$ ), longitudinal force ( $F_x$ ), normal force ( $F_z$ ), aligning moment ( $M_z$ ), inflation pressure and friction coefficient. All of which are very important parameters for vehicle dynamics. However the estimation of these values is not presented within the context of this work.

Two low cost data acquisition systems were designed in-house with two different Arduino platforms. However these fell short of data acquisition performance requirements required for realistic driving applications. It was seen that the Arduino family, low-end microprocessors, were not the best choice for applications of this nature. Finally electronic improvements such as the usage of field programmable gate arrays (FPGA) is discussed and suggested for future works.

## **Acknowledgements**

I would like to thank Professor Amir Khajepour for his endless wisdom, guidance and patience throughout my entire journey.

I also would like to thank all my friends and family for their support, joy and laughter during my studies.

## Table of Contents

AUTHOR'S DECLARATION .....	ii
Abstract .....	iii
Acknowledgements .....	iv
List of Figures .....	vii
List of Tables.....	viii
Nomenclature .....	ix
Chapter 1 Introduction.....	1
1.1 Motivation of the Project.....	1
1.2 Objectives of this Research .....	3
1.3 Distribution of Research Work and Individual Contributions.....	3
1.4 Thesis Outline.....	3
Chapter 2 Literature Review .....	5
2.1 Tire Models .....	5
2.2 Smart Tire Systems .....	6
2.2.1 General Approach.....	6
2.2.2 Sensory Technologies for Smart Tires .....	6
2.3 Data Acquisition from High Speed Rotating Devices.....	11
2.4 Low-Cost DAQ Systems .....	12
2.5 Energy Harvesting.....	13
Chapter 3 Smart Tire System .....	15
3.1 Need for a Smart Tire .....	15
3.2 Design Objectives.....	16
3.2.1 Data of Interest .....	16
3.2.2 Electrical System Structure & Requirements .....	18
3.2.3 Sensor Configuration & Requirements.....	19
3.3 Speed & Rotation Calculations for Data Sampling Rate Estimations.....	20
3.3.1 Fractional Distance based Data Sampling Rate Calculation .....	22
3.3.2 Angular Based Data Sampling Rate Calculation.....	22
3.3.3 General Formulation.....	23
Chapter 4 Data Acquisition System .....	24
4.1 High Level System Design.....	24

4.2 Software Flow Chart of the DAQ System .....	25
4.3 Mechanical Requirements of the System.....	27
4.4 Sensor Selection.....	28
4.4.1 Strain Gauges .....	28
4.4.2 Optical Sensors .....	28
4.4.3 Piezo Based PVDF Sensor.....	29
4.4.4 Sensor Technologies Comparison Matrix.....	29
4.5 PVDF Sensor .....	30
4.6 Epoxy / Glue Selection Process .....	32
4.6.1 Sensor-Epoxy Durability Testing & Verification .....	34
4.7 Electronics Selection.....	39
4.7.1 Analog to Digital Converter (ADC) Selection.....	39
4.7.2 Microprocessor Selection.....	39
4.7.3 Mobile Data Storage Options.....	41
4.8 Battery Power System Design.....	42
4.9 Arduino DAQ Performance .....	44
4.10 Off-Shelf DAQ Selection.....	46
4.11 Signal Conditioning Circuitry.....	48
Chapter 5 Experimental Analysis .....	49
5.1 Road Testing & Experimentation .....	49
5.1.1 Road Data Collection.....	51
5.2 Filter Implementation in Matlab .....	53
5.3 Post Processing of Collected Data .....	54
5.3.1 Artificial Neural Network Design & Implementation.....	54
5.4 Arduino Based Data Acquisition Results.....	58
Chapter 6 Concluding Remarks .....	60
6.1 Summary .....	60
6.2 Future Works .....	61
Appendix A PVDF Data Sheet .....	62
Appendix B Electronics Data Sheets .....	63
Appendix C Arduino DAQ Schematics.....	64
Bibliography .....	65

## List of Figures

Figure 1 - Influence of Road, Vehicle and Tires on Overall Operational Characteristics [1] .....	1
Figure 2 - Experimentally Measured Longitudinal Tire Forces [2] .....	2
Figure 3 - Smart Tire System .....	16
Figure 4 - SAE Tire Axis System [35] .....	18
Figure 5 - Smart Tire Electrical System Block Diagram.....	19
Figure 6 - Smart Tire Sensor Configuration.....	20
Figure 7 - Sample Tire Physical Model for Data Sampling Rate Calculations .....	21
Figure 8 - Smart Tire Monitoring System High Level Block Diagram.....	24
Figure 9 - Smart Tire DAQ Software Flow Chart.....	26
Figure 10 - IP Rating Standards [37].....	27
Figure 11 - LDT2-28K Piezo-based PVDF Sensor (Measurement Specialties Inc.) .....	30
Figure 12 - PVDF Sensor Electrical Model.....	30
Figure 13 - Crank-shaft Mechanism for Sensor and Epoxy Durability Testing.....	34
Figure 14 - PVDF Sensor Buckling Issue .....	35
Figure 15 - PVDF Sensor Creating a Dent into the Rubber Specimen .....	36
Figure 16 - PVDF Sensor Mechanical Practical Solution .....	37
Figure 17 - Oscilloscope Readings of the Modified Sensory Setup.....	37
Figure 18 - Fully Assembled Smart Tire Monitoring System .....	38
Figure 19 - Arduino UNO and Arduino MEGA ADK Development Platforms .....	40
Figure 20 - Adafruit SD Shield Expansion Card.....	41
Figure 21 - Arduino MEGA ADK with USB Stick for Data Storage .....	41
Figure 22 - Arduino Battery Pack Functional Block Diagram.....	42
Figure 23 - Smart Tire Monitoring System with DI-710 DAQ.....	47
Figure 24 - Smart Tire PVDF Sensor Buffer and Signal Conditioning Block Diagram .....	48
Figure 25 - Fully Assembled Smart Tire Monitoring System Installed on Chevrolet Equinox EV .....	49
Figure 26 - Waveform Capture Sample Obtained by DI-710 DAQ.....	51
Figure 27 - Signal Spectrum Analysis of PVDF Collected Data of 4Hz Excitation .....	52
Figure 28 - Signal Filtering Block Diagram.....	53
Figure 29 – Signal Filtering Results.....	54
Figure 30 - ANN Implementation High Level Block Diagram.....	55
Figure 31 - Sample Data from Load Wheel Sensor Collected by dSpace Platform.....	56

## List of Tables

Table 1 - Smart Tire Sensory Selection Matrix .....	29
Table 2 - Sampling Frequency Calculations for Various Sensing Lengths and Sampling Points for 40 km/h .....	31
Table 3 - Epoxy / Glue Testing Summary and Comparison .....	33
Table 4 - Arduino-based DAQ Performance Comparison and Evaluation .....	44
Table 5 - Off-shelf DAQ Comparison and Evaluation .....	46
Table 6 - Smart Tire Road Test Descriptions .....	50
Table 7 - ANN Performance Comparison & Evaluation .....	57



## Nomenclature

### Acronyms:

ABS	Anti-lock Braking System
ANN	Artificial Neural Network
CAN	Controller Area Network
DAQ	Data Acquisition
DC	Direct Current
FEA	Finite Element Analysis
FPGA	Field Programmable Gate Array
IP	Ingress Protection
LCR	Inductance (L), Capacitance (C), Resistance (R)
MIPS	Million Instructions per second
PC	Personal Computer
PCI	Peripheral Component Interconnect
PIC	Peripheral Interface Controller
PVDF	Polyvinylidene fluoride
SAE	Society of Automotive Engineers

SAW	Surface Acoustic Wave
SD	Secure Digital
SNR	Signal to Noise Ratio
SPDT	Single Pole Double Throw
Sps	Signals per second
TPMS	Tire-pressure Monitoring System
USB	Universal Serial Bus

# Chapter 1

## Introduction

### 1.1 Motivation of the Project

Tires generate the forces that drive and maneuver the vehicle. The knowledge of magnitude, direction and limit of the tire forces are essential and valuable for vehicle control and handling systems.

Tires are arguably one of the most useful device humankind has created. Before the implementation of rubber into the wheels, transportation was mainly carried out by wooden or metal tires attached to both horse-drawn and horseless carriages. However these tires provided significantly lower lateral forces due to their frictional capacities and hence the carts were only able to make turns at very low speeds. Lateral forces are crucial for vehicle steering and handling. Fortunately, with the introduction of rubber into the tires, higher lateral forces were reached and this lead to production of vehicles with better handling, steering and speed capabilities.

Outlined in Figure 1 below is the effect of tires, road and vehicle on environment, handling, safety, and comfort. It is seen clearly that the tires have a huge impact overall in every aspect of vehicle dynamics and count for a 20%-40% effect in handling performance.

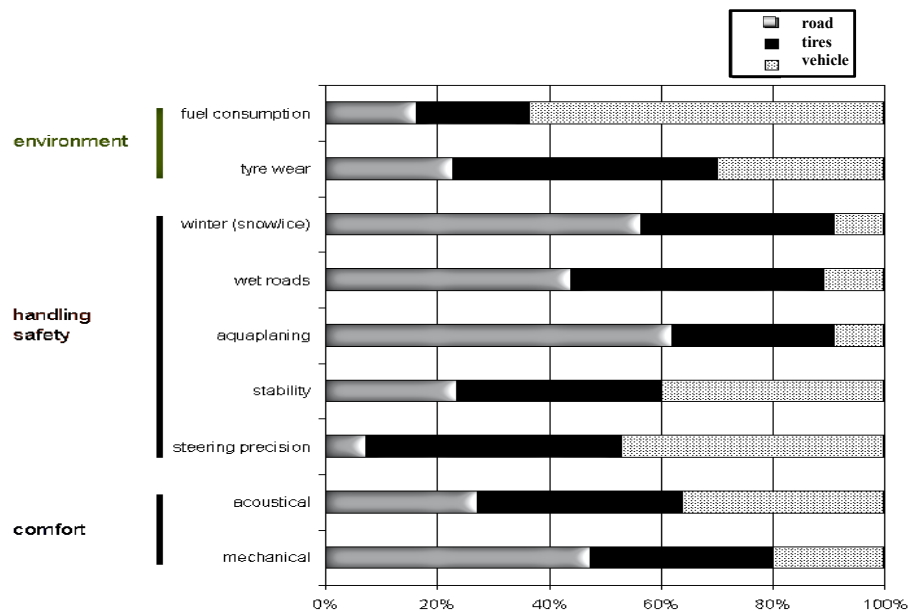


Figure 1 - Influence of Road, Vehicle and Tires on Overall Operational Characteristics [1]

To state briefly, rubber tires are very complicated units. The complexity results from not only the physical structure of the tire itself but is greatly affected by the chemistry of the tire making process as well.

Heat facilitates a polymerization reaction that crosslinks rubber monomers to create long elastic molecules. These polymers create the elastic quality that permits the rubber to be compressed into the surface area of the tire. In fact it is due to this chemical process that no two tires are alike on the molecular level. There is no means to measure and verify that the bonding took place properly and uniformly across the entire tire. For critical vehicle applications such as airplanes, the manufactured tires are X-rayed in order to validate good bonding [39].

This chemical complexity during the construction of the tires inherits itself in to the tire and results in a non-linear behavior of the rubber tire during normal operation. Tires are essentially sheets of reinforced fabric, steel wires and rubber. Their composition is not purely homogenous in terms of material properties. Although tires themselves may appear simple to an outside observer, their complexity makes them really hard to model in a linear fashion. Shown in Figure 2 is the experimental road data for a P225/60R16 tire [2]. The plot shows the braking force versus wheel slip ratio. 100% slip ratio means the wheel is locked, whereas 0% signifies that there is no slipping. Non-linear behavior of tire is easily observed in the plotted force curves.

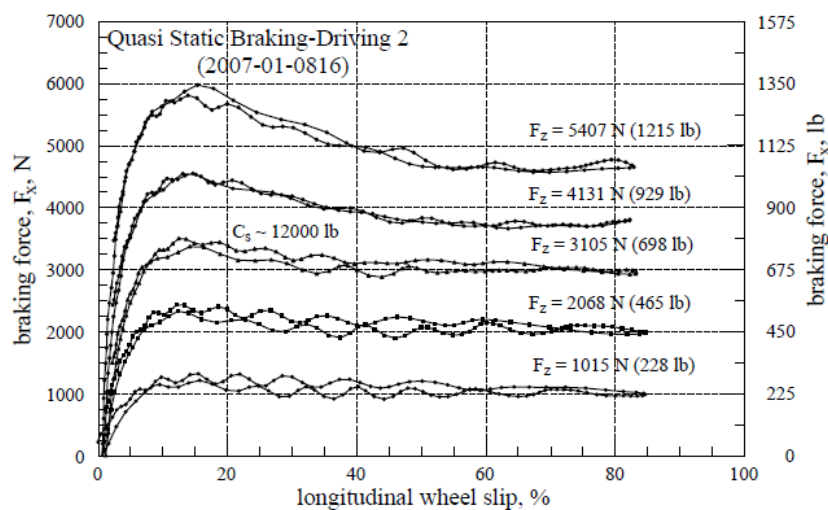


Figure 2 - Experimentally Measured Longitudinal Tire Forces [2]

The non-linearity of the tires makes them really hard to understand, simulate and analyze for design and performance evaluations. In order to have a more thorough understanding of vehicle dynamics, the huge importance of the tire forces should be realized and better analysis of tire forces should be pursued. Smart tires try to provide a better understanding of these tire forces by analyzing the pneumatic tire through different sensing and FEA modeling techniques.

## **1.2 Objectives of this Research**

The main objective of this project is to design and implement a data acquisition system that will collect incoming signals from the sensors in a rotating car tire during driving. The other objective of this project is to find a suitable sensor technology and epoxy pair that can be embedded inside a rubber tire to measure strain related physical data reliably and robustly. Once this is achieved, then important parameters such as lateral force ( $F_y$ ), longitudinal force ( $F_x$ ), normal force ( $F_z$ ), aligning moment ( $M_z$ ), inflation pressure and road friction coefficient can be computed from the collected strain data. All these values play an important role in vehicle dynamics.

## **1.3 Distribution of Research Work and Individual Contributions**

Due to the vast size and complexity, the research work for this project was divided between two students. A new FEA tire model had to be developed for this project and the work was carried by a PhD. candidate, Jennifer Bastiaan within the same research group [38]. This thesis however, thoroughly covers the electronics system that was designed and developed in order to collect relevant data to verify the developed FEA model. This thesis also covers the finding of a suitable sensor and epoxy pair to be implemented within the rubber tire for data harvesting.

Jennifer Bastiaan also did the assembly of the smart tire and sensor installations. She also put together the crank-shaft based testing mechanism to perform durability testing of the sensors.

## **1.4 Thesis Outline**

This thesis is structured in the following manner: Chapter 2 is the literature review and background. This chapter focuses on the current state of research in smart tires, strain sensors, tire force measurement systems, tire models and DAQ systems. Chapter 3 presents the proposed smart tire solution and gives a thorough description of the system concept and structure. The chapter also presents some calculations for estimating the optimal sensory input sampling rates for a desired

vehicle speed. Chapter 4 introduces the design of the DAQ system in detail. Spanning a very wide range, this section details all aspects of the DAQ system including sensory selection, epoxy selection, electronics design, system durability verification, and testing. This chapter also presents the comparison and adaptation of an off-shelf solution for acquiring data from a rotating car tire. Chapter 5 is dedicated to experimental results and analysis. Real road tests were performed and the proposed system successfully captured the strain related data. This chapter also expresses a few practical, yet simple ways to post-process the collected data through filtering and artificial neural networks. Finally, concluding remarks and future work are presented in Chapter 6.

## **Chapter 2**

### **Literature Review**

The small patch of tire that is in contact with the road is essentially the main element transmitting most of the forces acting on a vehicle. Tires in their essence carry vital information that can be used to understand the vehicle dynamics and this information can be further used in anywhere from driver assistance systems to ABS. Tire road friction and slip angle are considered to be the most significant variables affecting the response of the electronic stability control systems [35].

Due to the immense applicability of the topic in vehicle dynamics, the literature is filled with numerous attempts to model, measure and analyze tire behavior in various ways. This chapter aims to cover some of the published work among these approaches.

#### **2.1 Tire Models**

Accurate measuring of contact forces between tire and the road patch has been a field of deep research in the recent years. In [3], the author tries to measure some of these contact forces by correlating the strain information of the rim to the FEA model of the tire that they have developed. To do so, the study incorporates the installation of strain gauges on to the rim and the readings are then correlated to the FEA model. Author shows that his method is successful in measuring the vertical load, side slip angle and wheel torque values.

The authors in [4] use a piezo based sensor to measure the deflections of the tire sidewall. Then this information is fed into their FEA model and the correlated tire side slip angle value is computed. Authors have also developed their in house testing rigs and have performed experimental runs to verify their model. For data transmission, they have simply converted the voltage coming from the piezo sensor to frequency modulated radio signals and have used a transmission data rate of 4.2 kHz. However, their proposed system was not tried in a real road driving test.

In [5], the authors have embedded a flexible pressure sensitive electric conductive rubber (PSECR) sensor inside the tire surface. This sensor is capable of measuring multi-dimensional compressive forces and the collected values are then fed into a tire model based on a beam-spring model. By doing

so, the authors have demonstrated that their techniques, along with the tire model can be used to estimate multi-dimensional load friction values for automobiles. In order to test the validity of their approach, the authors used a laboratory testing rig and a motorcycle tire for experimentation.

In [6], the author used numerical estimation techniques and extended Kalman filters based on the tire model to estimate the forces between the tire and the road. The results of their simulations indicate that the author was able to calculate the friction coefficient and side slip angles within reasonable accuracy. In order to test their approach, the author compared the performance of the developed system against a real car equipped with a load wheel. A load wheel is capable of measuring all wheel forces and moments on a vehicle tire [40].

## **2.2 Smart Tire Systems**

### **2.2.1 General Approach**

Although the idea of a “Smart Tire System” and the obvious need for it are discussed in Chapter 3, literature study suggests that this has been a topic of great interest for numerous years.

A research team funded by the European Community, along with some major tire companies, worked on the project APOLLO – “Intelligent Tire for Accident-free Traffic” [7]. As a part of this project, APOLLO has released a very thorough study of the intelligent tire systems covering all the aspects from the available sensory technology to data transmission methods, entitled “Intelligent Tyre Systems”. APOLLO project by itself shows the immense demand and support from the automotive industry for the development of smart tire systems. Simply put, this project explores various sensing ideas such as capacitive strain sensors, 3D accelerometers, and optical displacement sensor to analyze the behavior of the tires. One of the many conclusions that the authors draw is that the capacitive based strain sensing is the most applicable and affordable sensory method available for smart tires today.

### **2.2.2 Sensory Technologies for Smart Tires**

There are numerous sensory technologies available for collecting strain and deflection related data from tires. Some of the examples are piezo-electric PVDF sensors, capacitance based strain sensors,



resistance based strain sensors, surface acoustic wave sensors, and fiber Bragg grating. Some of these approaches are evaluated in the following paragraphs.

#### **2.2.2.1 Piezo-Electric Sensors**

A promising, yet preliminary publication [8] uses PVDF based piezoelectric sensors to analyze tire rubber deformations. This information is then used to analyze the friction characteristics between the wheel and the ground. They attached two PVDF sensors inside the tire along the centerline. Sensors are glued such that the deflection occurs only in longitudinal x-axis. To prove their concept, the authors used a skid-steered mobile robot for experimental verification. This data was then transmitted wirelessly to an onboard computer. Their experimental results indicated some success in their approach; however they were limited at 100 Hz sampling rate for their data collection. As it will be discussed in the Chapters 3 and 4, this sampling rate would not be enough to analyze the behavior of automobile tires at traveling speeds above 20km/h.

A thorough study, [9] focuses on the behavior of dynamic signal in a PVDF sensor; and evaluates the PVDF sensor durability. Though very informative, their study confirms the applicability and behavior of PVDF based sensors in deflection measurement applications. The authors tested the sensors up to 360 minutes of successful operation.

#### **2.2.2.2 Rubber Based Sensors**

Since the Young's modulus of rubber is very low, 0.01-0.1 GPa [41], it is not suitable to use foil based strain gauges to measure surface strain [10]. De-bonding as well as sensor damage is inevitable for long duration applications. Multiple works have been analyzed in this field where the authors tried to design a flexible rubber based sensor that can withstand the high elasticity of a rubber tire.

The author in [10] presents the design of a rubber based strain sensor using photolithography. Similar to the previous approaches, the sensor presented in this study measures the capacitive changes between its electrodes. In their study, the authors fatigued the new sensor over  $10^6$  cycles and found that the sensor was still fully operational. They were able to successfully measure strains levels applicable to rubber tires. The excitation force applied to the tire was created by a testing machine with controlled stroke speeds. In their study the author uses a bulky LCR meter for the capacitance analysis, which makes this approach tricky for real automobile applications.

Coming from the same author and his colleagues, [11] is another approach for the fabrication of a flexible strain sensor based on flexible polyimide substrates and a highly flexible epoxy resin. Similar to the previous approaches, this sensor aims to measure the capacitance changes between its carefully patterned electrodes. Having an elongation of 150%, the epoxy resin was found to be a very promising substrate for flexible sensor applications. This study also looks at the effects of temperature on the capacitance of the rubber tire and states that temperature compensation needs to be considered for the future, if accuracy is crucial. The authors went a step further by incorporating wireless data transmission from the sensor using amplitude modulation, similar to the technology used in our daily radios. By using a simple transmission circuitry, the authors successfully transmitted the capacitance readings to a nearby oscilloscope where the signals were collected. Then the analysis was performed on a PC.

### **2.2.2.3 Sensorless Methods – Capacitive and Resistive Electrical Properties of Tire**

A review of the related literature suggests that a noticeable amount of work has been done where the rubber tire itself is used for analysis with no need for additional sensory. Most of the approaches taken in analyzing the road-tire interaction use the capacitive and resistive properties of the tire itself. Logic might assume that these methods are somewhat intrusive. Rubber of the tire had to be scraped off in order to connect electrodes to the steel wires in the carcass. This might inevitably decrease the lifetime of a rubber tire.

In [12], the author tries to measure the mechanical deflections of a tire by analyzing the capacitive-resistive behavior of the rubber tire. The analysis takes place by looking at the impedance changes between the steel wires inside tire carcass. In order to do so, the authors removed rectangular strips from a rubber tire, and attached electrodes onto two adjacent steel wires. After modeling the tire structure as a big capacitor array, the experimental response of the system was analyzed by an LCR meter for displacement excitations. Their studies suggest that their approach resulted in linearity about 84%. In other words, their study found a promising correlation between the capacitance of the steel wires and the strain values of the tire. More so, they extended their study by analyzing the effects of temperature on the tire specimen as well. Notice must be taken for the fact that temperature has a noticeable effect on the capacitive tire model. This key concept seems to be missing in most of

the studies that aim to develop measuring means based on rubber capacitance. However, their approach shows that the capacitive and resistive properties of the tire itself can be used for tire-road deformation analysis.

In [13],[14],[15],[16] all published by the same author propose numerous design solutions to use the capacitance, electro-magnetic properties and resistive properties of the steel wires inside a rubber tire carcass for surface strain measurements. All of the proposed solutions are sensorless, i.e. they use the information readily available within the tire rubber. Intrusive it may be as all these solutions require scraping off the surface of the tire in order to access the steel belts; the author and his team show numerous reliable ways to measure the strain data from a rubber tire. Some of these studies do mention the effects of the temperature and try to compensate for the effects by using circuit elements like the thermistor.

Following their previous works, the same author also analyzed the multiple spectral features of the capacitive-resistive behavior of the rubber tire [17]. By the addition of probability into the system by using signal spectrum analysis, the authors were able to come up with a more reliable way to passively measure the strain of the tire than the aforementioned works. By using the relation between applied strain and spectral features, the authors came up with multiple regress functions that can accurately correlate to the strain of the tire. The estimations carried out were very accurate and through model reductions, their model was able to calculate the tire strain based on the spectral values of three variables, namely tuning frequency, peak power spectrum and the quality factor.

#### **2.2.2.4 Other Sensory Technologies**

Aside from the flexible sensor approaches such as the rubber based or PVDF, there have been numerous studies where the authors came up with really inventive ways to analyze the strain and surface contact patch contours of rubber tires.

In [18], the author introduces the usage of SAW sensors. These passive sensors are excited by applying a radio signal. Once excited, the sensor outputs a surface acoustic wave and this response can be read and analyzed to extract displacement data. The authors came up with a very creative way which involves embedding a pin-lever into the rubber tire. The ball head of this pin is then placed on the SAW sensor. As the tire rotates, and the pin is deflected, the corresponding displacement of the

pin head was captured and transmitted by the SAW sensor. Intrusive though it may be to the structure of the tire, their proposed solution was successful in capturing tire strain data in a stationary laboratory testing rig at speeds up to 140 km/h.

In [19], the author puts forward the usage of highly sensitive 3D magnetic field sensors to be used in intelligent tires. This sensor houses five Hall Effect sensors that are interconnected to each other. Through the correlations, the sensor is capable of measuring the magnetic field changes in all 3 (x-y-z) dimensions. By embedding a permanent magnet inside the tire, and placing the 3D magnetic field sensor beneath it, the published work aims to measure the rubber displacement. Authors claim that the proposed sensor is more reliable and more sensitive than the other available 3D magnetic field sensor solutions. Interesting it may be, it still isn't clear how the authors aim to use this in an intelligent tire application since their work does not present any experimental analysis with the proposed sensor inside a tire.

Author in [20] tries to implement 3-axial MEMS based accelerometers inside a tire in order to measure contact forces and patch features. They place three sensors inside a tire, and by correlating the readings to a FEA model, they claim to successfully measure numerous parameters from the tire such as side slip angle and normal force. Their lab experiments were performed on developed machinery, MTS Flat Trac III [42].

A fiber Bragg grating (FBG) is a reflector constructed in a short segment of optical fiber. It reflects certain wavelengths and transmits all the others. By looking at the phase changes in the reflected laser, it is possible to measure the displacement of the specimen surface. In [21], the author proposes fiber Bragg grating to measure strain. Being lightweight, immune to electromagnetic interference and light, fiber Bragg grating offers the ability to measure very high strain elongations. However, the cost of this system is well beyond that of a fancy sports car. Needless to say, it is not applicable to be used as a feasible solution for smart tire systems.

The author in [22] proposes a new method to measure the shape and strain distribution of a tire by using optical means. In their approach, the authors utilized 2D phase analysis using phase-shifting Moiré patterns. To do so, the authors attached a grating pattern on a rubber tire and optically analyzed

the strain changes through two CCD cameras. Their model and approach was successful in measuring the 3D shape and strain distribution of a tire rotating at 80 km/h.

Another optical based, non-contact strain measurement system for rubber tires is presented in [23]. In this work, some of the image manipulation techniques such as blurring were used. Through his approach, the author produced strain distribution maps of the tire contact patch. However one of the limitations faced was the limited resolution of the camera. Also it was seen that, the optics (i.e. lenses) required for the system to work properly had some limitations in terms of reliability. Alignments of the optics were found to be deviating at times and this caused problems with the data accuracy. Simply put, the presented system is able to do strain analysis of a rubber tire but yet falls short of being a complete solution for the needs of the smart tire systems.

### **2.3 Data Acquisition from High Speed Rotating Devices**

So far most of the studies done in the field were found to be only indoor laboratory bound, that is the sensory data collection systems were never used in real driving conditions. One big question that comes to mind is the performance and reliability of data acquisition systems in remote and rotating environments. For instance, what happens to a wireless transmitted signal, if the source happens to be a rotating frame? Does it get distorted, does the SNR ratio change? Questions of these sorts have been answered, in numerous works.

In [24] for instance, the author studies the electromagnetic wave propagation characteristic properties in rotating environments. As shown in their work, wireless signals tend to differ when the signal source happens to be on a rotating frame. Simply put, there is a noticeable amount of increase in signal path losses. In this study, the authors also analyzed the signal quality of the transmitted TPMS sensory readings over wireless transmitter while driving the car with speeds up to 120 km/h. Even though none of their approach is directly applicable to real world smart tires as their data collection sample rate was 4s, and transmission took place once in every 10s, it still shows the feasibility of a stable wireless communication channel between a rotating tire and a stationary control unit.

In [25], researcher looks at the rotating speed dependent wireless data package transmission error rates. Their study is interesting in the sense that it presents a very thorough analysis of wireless signal behavior for rotating systems. Their conclusions support the feasibility of the smart tire, as the

wireless transmission systems were proven to be applicable in rotating environments. In their research, the authors pushed the limits of the rotating speeds all the way up to 1900 rpm, which is equivalent to ~250 km/h. Even at these really high speeds, the wireless transmission system successfully produced reliable results.

Author of [26] focuses on the analysis of data acquisition system reliability for a very high speed rotating application used in mining industry. Although their proposed solution uses slip rings and is not directly applicable to the sought after smart tire application, it still is a promising step to show the reliability of data acquisition systems in rotating environments. In their research, the authors tested the functionality of the data collection systems for rotating speeds up to 1050 rpm, which translates to a speed of 140 km/h on a car. The authors found out that due to the immense amount of data, using an FPGA based electronics system turned out to be a better choice than using low cost microprocessors such as PICs or microcontrollers.

## **2.4 Low-Cost DAQ Systems**

Another important aspect of this thesis was to come up with a reliable DAQ system to be used in smart tire analysis that is also not very expensive to be implemented. Numerous works have been done in the area of low cost DAQ designs. Some of these works were also reviewed.

In [27], the author proposes the design of a DAQ system that uses PCI interface for PC communication. Their system houses a Xilinx FPGA as the main processing unit along with a 200 MSps ADCs from Analog Devices. Even though being a PCI interfaced solution makes this approach not so practical for smart tire applications, it still shows very promising methodology to achieve DAQ rates of 200 MHz, with real time FPGA processing speeds up to 4000 MIPS. This sort of data acquisition rates are well above most of the readily available off-the-shelf DAQ solutions which are priced for \$1000 or less.

Presented in [28] is a very interesting approach where the author utilizes an Android smartphone and use it as a data acquisition system. To do so, they capture the 3D accelerometer data coming from the smartphone which is attached to the collar of a dog. Apparently this sort of information is useful for doing gait analysis for dogs. In order to capture the data on the phone, the authors used an application which is freely available in Android app store. Sadly, their sampling rate is capped at 100 Hz. This

value is a hardware limitation of the smart phone itself and therefore limits the usage of this low-cost solution in high speed data acquisition for smart tire monitoring systems.

Most of the DAQ solutions studied were found to be using proprietary acquisition software. These sometimes happen to be the bundled software packages that come along with the digital oscilloscope or the LCR analyzer themselves. However for a custom built smart tire application, it would be preferable to build one's own software interface or even better use an open source solution. In [29] the author attempts the latter by utilizing an open source DAQ system called OpenDAQ. This DAQ is capable of capturing data at 20 KHz sampling frequency split over 8 single-ended channels. Being open source, this work remains to be a great guideline for designing custom built DAQ solutions in terms of software design.

PARduino is an inexpensive data logging solution built on Arduino Pro Microcontroller [30]. The support of the open-source community made the Arduino development platforms fairly popular in the recent years. In this paper, the authors developed the Arduino based system to collect radiation related data from the nature for forestry applications. Although the sampling periods were at 10 hours, the project remains to be a good example where a low cost Arduino board was used as a standalone SD-Card data logger. As will be discussed in Chapter 4, the same platform was studied in this thesis as well.

## **2.5 Energy Harvesting**

If smart tires were ever to become everyday household items one day, it is quite rational to presume that energy harvesting from the tire itself would also be an important area of interest. Ideally, a perfect smart tire system should be able to harvest its own electrical energy from the rotation of the tire, and use this stored charge to transmit the read data. There have been a few approaches for harvesting energy from rotating tires.

In [31] and [32], the authors use essentially the same idea, that is they use the gravitational pull on the rotating tire frame on a pendulum to generate electricity. Similar to the hydroelectricity generation, the gravitational pull on the tire makes the pendulum system an energy harvester once hooked up to an ordinary DC motor. Even though both papers do succeed in generating power through their pendulum approach, the RMS of the voltage created falls short for operating any electronics to

acquire data. The generated voltage through these systems happens to be within only 70-100mV range. In fact in [32], the author concludes by stating that only 10% of wheel rotation can be effectively used for power generation.

Instead of using the gravitational pull on a mass attached pendulum [33] and [34] use piezo-electric beams to harvest energy from rotating tire. Research done in [33] is particularly interesting where the author designs a piezo-based strain sensor that harvest its own energy to transmit data. However in [34], the author just aims to harvest to generated voltage by the piezo-electric beam. Even though similar to the aforementioned methods, none of these methods achieves the voltage levels required to run a stand-alone DAQ system on a tire.



## **Chapter 3**

### **Smart Tire System**

The operational properties of a road vehicle are the result of dynamic interaction of the various components of the vehicle structure. A major role is played by the pneumatic tire. In addition, tire characteristics are of crucial importance to the dynamic behavior of a road vehicle.

#### **3.1 Need for a Smart Tire**

The importance and huge influence of the tires have long been accepted and numerous incentives have been introduced to attract more attention into the design of smart tire systems. Put forward by the APOLLO project [7], below are the three major objectives of a smart tire system.

1. To increase traffic safety by adding an intelligent tire/wheel system to advanced vehicles which provides data on the particular tire and the given tire-road contact
2. To enable improvements for chassis/vehicle control systems, Advanced Driver Assistance Systems (ADAS), and driver information
3. To enable the introduction of innovative services concerning tire and road conditions for different user groups outside the vehicle

As stated numerous time in the APOLLO project, the main goal of the smart tire system is to increase the traffic safety overall. By gaining a deeper understanding of the pneumatic tire and by monitoring real-time behavior of the tire itself, it is believed that a more thorough vehicle system dynamics and control thereof can be established.

The remainder of this chapter will cover the proposed smart tire monitoring solution. While this chapter will aim to deliver the main aspects of the proposed system, the detailed design of system components will be introduced in Chapter 4.

### 3.2 Design Objectives

Seeing as the APOLLO objectives do cover a very broad spectrum of applications, the sought after objectives for the smart tire system presented in this project had to be established. As described in the introduction section, a considerable amount of research work has been carried out by Jennifer Bastiaan as her PhD. thesis in smart tires [38]. Some of the objectives presented in 3.2.1 were initially highlighted within her work.

#### 3.2.1 Data of Interest

The aim of this study is ultimately to be able to extract the strain information of a rotating tire. If done accurately, the following parameters can be computed. All these parameters play an essential role in the overall multi-body dynamics of a road vehicle as well as vehicle control dynamics. Summarized in Figure 3 below are the desired outputs of a fully functional smart tire system.

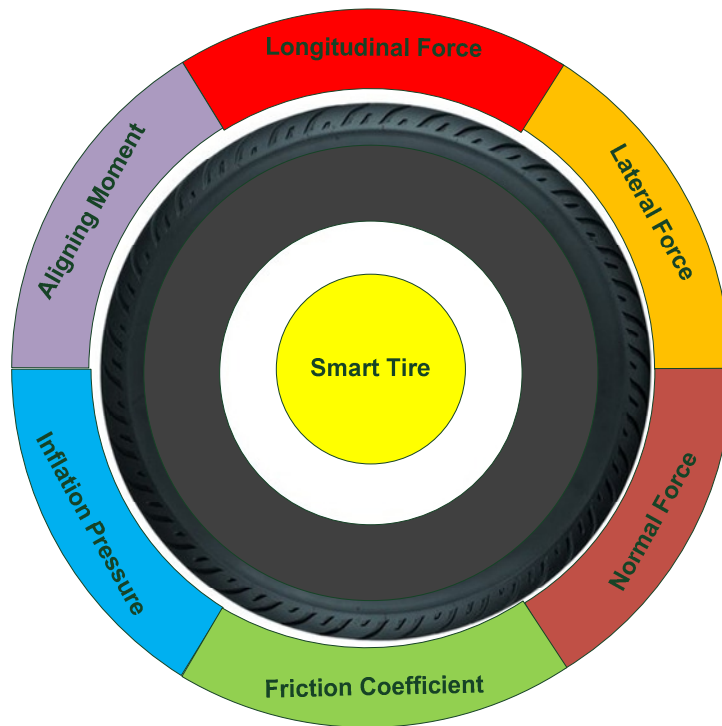


**Figure 3 - Smart Tire System**

Longitudinal Force ( $F_x$ )- Longitudinal motion is mostly excited during acceleration and deceleration. This motion is the most important factor determining the performance behavior of a vehicle. Positive longitudinal force is named tractive force, while negative is named braking force. This force is generated due to shear stresses at the contact patch and is in x-direction.

Lateral Force ( $F_y$ )- Lateral motion is a force along y-axis and is excited mostly during steering and cornering. This motion is important particularly in vehicle handling. This force is the main cause of sideslip. This force is generated due to shear stresses at the contact patch and is in y-direction.

Normal Force ( $F_z$ )- Also known as the holding force, is the force along the z-axis. The magnitude of this force is directly related to the vehicle road holding and indirectly related to vehicle handling and performance.

Friction Coefficient ( $\mu$ )- This value defines the properties of the physical mediums that are in contact between the tire and the road. All contact (shear) forces are generated from this physical contact.

Inflation Pressure- For ride safety, comfort, vehicle performance and handling, inflation pressure is an important factor.

Aligning Moment ( $M_z$ )- This moment is about the z-axis and is the force that tries to resist the wheels turning from steering. It is mostly applied in negative direction and affects the vehicle handling and stability, however not in great amounts.

Figure 4 shows the aforementioned forces in SAE's tire axis system.

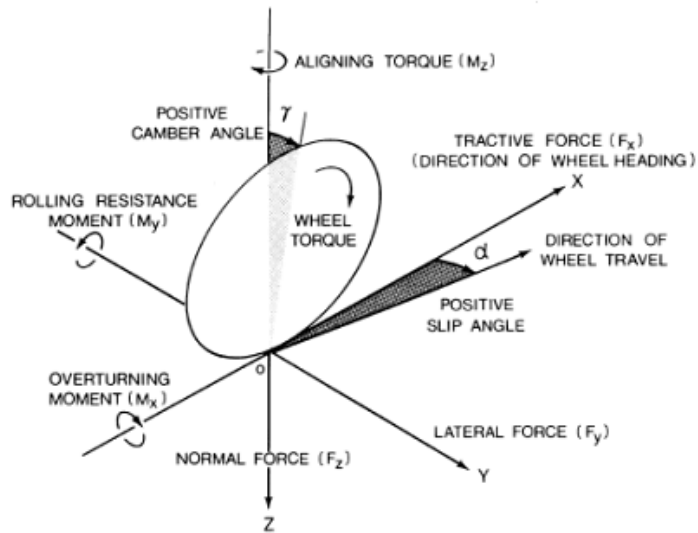


Figure 4 - SAE Tire Axis System [35]

### 3.2.2 Electrical System Structure & Requirements

Assuming a smart tire system is capable of successfully capturing afore mentioned data, the data acquisition instrumentation of the system still needs to fulfill various other requirements such as:

- The overall system should be robust enough to withstand a rotating environment
- The system should be water and dust tight for harsh driving conditions
- The system should reliably capture and store tire sensor data with no user intervention required
- The system should be self-powered and its battery should last for at least a few hours
- The system should have adequate amount of storage capacity in order to be used in extensive testing scenarios
- The collected data should be stored on board on removable medium and be extracted later for post processing. Data should be time labeled properly to identify the test counts as well as separate sensor channels
- System should house a power switch and status indicator LEDs
- The system should be reasonably priced (<\$500). This applies both to data acquisition electronics as well as sensory to be used
- The system should also be light (<5 kg). If too heavy, inertia forces could damage the data acquisition system, also the weight balance of the wheel might get altered as well
- Design of the system should be flexible enough to leave room for improvements in the future, such as wireless data transmission, CAN communication and energy harvesting

Shown in Figure 5 is a top-level system structure for the data acquisition system to be utilized in smart tire for experimental analysis.

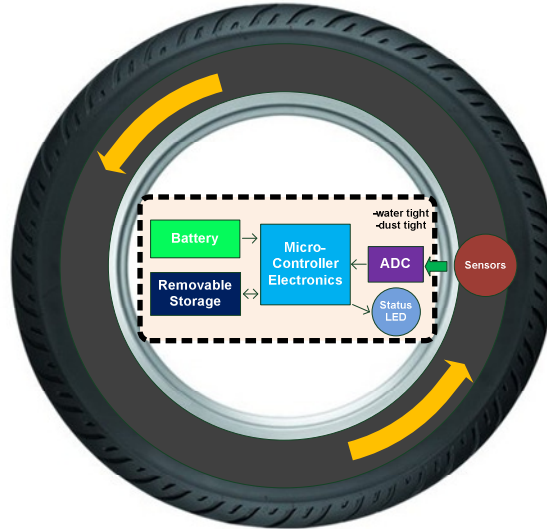


**Figure 5 - Smart Tire Electrical System Block Diagram**

### 3.2.3 Sensor Configuration & Requirements

Based on the tire FEA model developed by Jennifer Bastiaan [38], it was determined that using the strain information of 6 points around the ground contact patch was sufficient to correlate the collected strain data to the tire model to extract the parameters described in 3.2.1.

Figure 6 illustrates 4 out of 6 sensor locations of interest inside the tire. The remaining two sensors placed inside the tire, on left sidewall, are not shown. By collecting the strain related sensory data from all 6 channels simultaneously, the dynamic behavior of the tire can be analyzed through soft intelligence based computation techniques such as artificial neural networks.

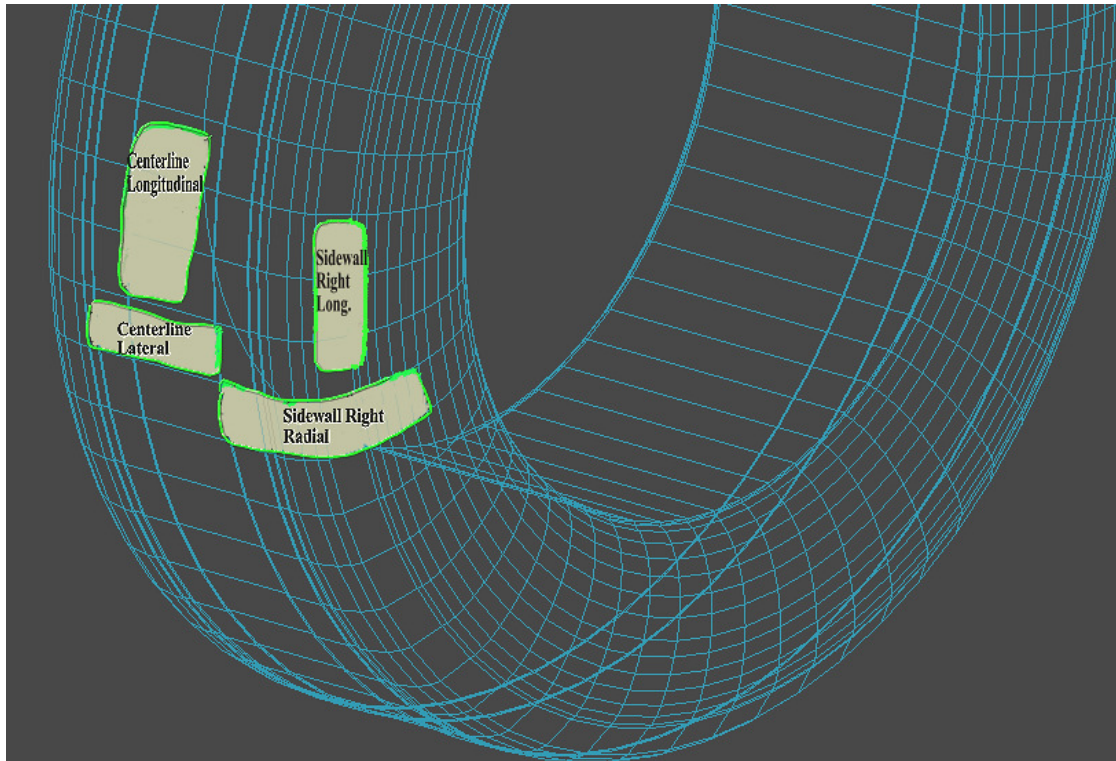


**Figure 6 - Smart Tire Sensor Configuration**

Similar to the electronics, the desired smart tire sensor should be able to meet certain requirements.

Listed below are these in no particular order.

- Sensor should be flexible so that it can reliably measure strain related information on rubber surface with very low Young's modulus
- Sensor should be light (<5 g) enough to not interfere with rotating wheel dynamics. If sensors are very heavy, the weight balance of the wheel might get affected
- Passive sensing is more desirable. Simply put, passive sensors are easier to integrate into harsh working conditions since they don't require additional power source
- The sensing material should be coated with sufficient protection so that a suitable epoxy can be applied to attach the sensor on tire walls without damaging its electrical properties
- Sensor should be reasonably priced (<\$15) for mass production
- Sensor should be robust enough to withstand the long life duration of an average medium size car tire (2 years / 100000 km)

### **3.3 Speed & Rotation Calculations for Data Sampling Rate Estimations**

So far the main requirements of the desired smart tire experimental analysis system have been described. Another key point to consider in the system design phase is the desired throughput of the data acquisition system. To do so, some crude calculations were performed to understand what the

desired data acquisition rates should be for the smart tire analysis. Desired data acquisition rates are the sampling rates which capture sufficient amount of data points at a given car speed to reliably estimate the data of interest described in 3.2.1.

One important factor that affects data sampling rates is the vehicle speed that the data captures are performed at. Since most of the initial system testing would be performed on University of Waterloo's ring road, 40km/h, the speed limit thereof has been used as worst case condition. Put simply, the designed data acquisition system should be functional at speeds of at least 40km/h.

Another important factor affecting the sampling rate is the desired amount of data required for the soft intelligence computing tools to work reliably. There are two approaches that can be taken for calculating the ideal sampling rates. Both methods are presented. Firstly, basic wheel frequency is calculated based on Figure 7 below.

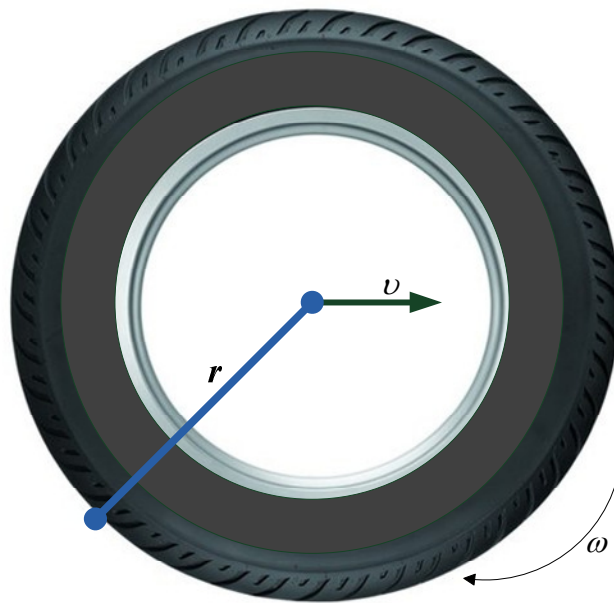


**Figure 7 - Sample Tire Physical Model for Data Sampling Rate Calculations**

Where;

- $r = 0.35\text{m}$  (18-inch Midsize Car Tire)
- $v = 40 \text{ km/h}$

The traveled distance per one wheel revolution is equal to the circumference the wheel and can be calculated as;

$$\text{Circumference} = 2 \pi r = 2.2 \text{ m} \quad (1)$$

Therefore the wheel frequency can be shown as;

$$40 \text{ km/h} = 11.1 \text{ m/s}$$

$$\text{Wheel Frequency} = \frac{11.1 \text{ m/s}}{2.2 \text{ m}} = 5 \text{ Hz} \quad (2)$$

### 3.3.1 Fractional Distance based Data Sampling Rate Calculation

Now that the wheel frequency is known, Equation 3 below is the period and frequency of each 1cm of tire longitudinal travel.

$$T_{fd} = \frac{0.2 \text{ s } 1 \text{ cm}}{220 \text{ cm}} = 9.09 \times 10^{-4} \text{ seconds} \rightarrow f_{fd} = \frac{1}{9.09 \times 10^{-4}} = 1.1 \text{ kHz} \quad (3)$$

In Equation 3,  $T_{fd}$  is the time period of 1 cm of wheel longitudinal travel and  $f_{fd}$  is the corresponding frequency. In other words, the car wheel travels 1cm 1100 times a second.

### 3.3.2 Angular Based Data Sampling Rate Calculation

Now that the wheel frequency is known, Equation 4 below is the period and frequency of each 1 degree of tire angular rotation.

$$T_{ab} = \frac{0.2 \text{ s } 1 \text{ deg}}{360 \text{ deg}} = 5.56 \times 10^{-4} \text{ seconds} \rightarrow f_{ab} = \frac{1}{5.56 \times 10^{-4}} = 1.8 \text{ kHz} \quad (4)$$

In Equation 4,  $T_{ab}$  is the time period of 1 degree of wheel revolution and  $f_{ab}$  is the corresponding frequency. In other words, the car wheel hub turns 1 degree 1800 times a second.

At this point, it should be realized that both of the values calculated above were for one data sample point. The acquisition frequency to capture  $N_{samples}$  of information per 1 cm unit distance, and 1 degree angle for 40 km/h are shown in Equation 5&6;



$$f_{fd@40km/h} = 1.1 \text{ kHz } N_{samples} \quad (5)$$

$$f_{ab@40km/h} = 1.8 \text{ kHz } N_{samples} \quad (6)$$

### 3.3.3 General Formulation

Equations 5&6 can be further expanded to the following form where all system variables are incorporated into the sampling frequency calculations.

$$f_{fd@vkm/h} = \left[ \frac{v}{3.6x} \right] N_{samples} \text{ (per each } x \text{ m of tire surface)} \quad (7)$$

$$f_{ab@vkm/h} = \left[ \frac{50}{x} \right] \left[ \frac{v}{\pi r} \right] N_{samples} \text{ (per each } x \text{ deg of wheel revolution)} \quad (8)$$

where;

$v$  = velocity of vehicle [km/h]

$r$  = wheel radius [m]

$N_{samples}$  = # of desired samples for capture

$x$  = value of interest

The two derivations above will be used to compute the desired data sampling rate once the sensor is selected and its mechanical dimensions are counted for.

## Chapter 4

### Data Acquisition System

So far the main aspects of the required smart tire monitoring system, such as the electrical and operational requirements, and desired data sampling speeds have been identified. This chapter will present the design of the data acquisition system in detail.

To do so, first the overall high level system will be discussed. Secondly, the flow chart of the system software will be introduced. The physical and mechanical needs of monitoring system will also be addressed. Then to follow, a “bottom-up” design strategy will be applied for sensory selection, epoxy selection, electronics selection and signal conditioning designs.

#### 4.1 High Level System Design

Shown in Figure 8 is the block diagram of the data acquisition system. The requirements of the sought after system have already been identified in Chapter 3.

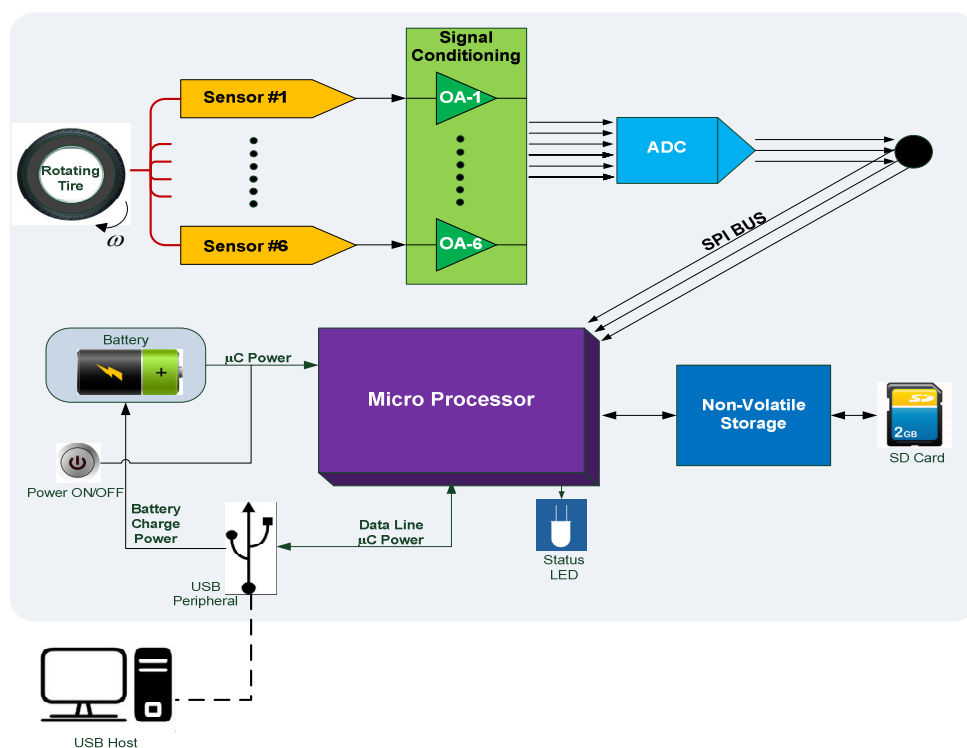


Figure 8 - Smart Tire Monitoring System High Level Block Diagram

To better understand the flow of the entire diagram shown in Figure 8, given next is a description of the smart tire monitoring system in action:

The incoming information from the sensors that are attached to the inside of a rotating tire will give out strain correlated readings. These signals will first be conditioned through an op-amp based signal conditioning circuitry. Then these signals will be acquired through an analog to digital converter (ADC) and the converted values will then be fed into a microcontroller through serial (SPI) interface. The microcontroller will write the collected data onto a non-volatile SD card. Once this requirement is met, then other design possibilities such as writing data to a USB stick, and data transmission over Ethernet/Wi-Fi can also be considered.

USB interface is used both for charging the battery and also establishing data communication with the microprocessor. This dual functionality of the USB is similar to that of smartphones and tablets where one plug is sufficient for both data transmission and battery charging needs.

## **4.2 Software Flow Chart of the DAQ System**

It is reasonable to say that the software design of the smart tire monitoring system is not very complicated and fairly straight forward. All the system is asked to do is to collect and record acquired data during normal operation. Shown in Figure 9 is the software flow chart describing system operational behavior.

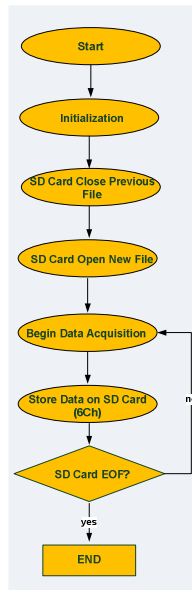


**Figure 9 - Smart Tire DAQ Software Flow Chart**

When the system is powered up, first the electronics get initialized. In order to provide reliable functionality, SD Card needs to be forced to close its previous file. Once this is achieved, a new file is created and opened on the SD card and the data acquisition begins to acquire and write data into this file. The device keeps recording the data until the End of File (EOF) is reached on the SD card. It was seen that this simple software approach minimized the amount of user intervention required for reliable system operation.

### 4.3 Mechanical Requirements of the System

Since the smart tire monitoring system is to be used in a remote and harsh environment, several mechanical requirements need to be met.

First and foremost, the designed data acquisition system should reliably operate in a rotating environment. This essentially is how well the system is “packed” into its housing. Anything loose within the system box will eventually bounce around and potentially cause damage to the rest of the electronics. Designed data acquisition system is to be mounted on a rotating wheel. It should be reasonably sized and must also not weight too much (<5 kg) to interfere with the wheel’s balance.

In order to make the system more robust and operational in numerous driving and weather scenarios, the system box will be designed to comply with the IP standards. For this project, IP-68 standard was chosen. Shown in Figure 10 is a detailed description of the IP standard ratings.

1 <sup>st</sup> Digit	Symbol	Solid Object Protection	2 <sup>nd</sup> Digit	Symbol	Water Protection
0		Not protected	0		Not protected
1		Protected against solid objects greater than 50mm	1		Protected against vertically dripping water
2		Protected against solid objects greater than 12.5mm	2		Protected against dripping water when tilted up to 15°
3		Protected against solid objects greater than 2.5mm	3		Protected against spraying water
4		Protected against solid objects greater than 1.0mm	4		Protected against splashing water
5		Protected from the amount of dust	5		Protected against jetting water
6		Dust tight	6		Protected against powerfully jetting water
<p style="text-align: center;"><b>IP 6 6</b></p> <p>Code Letters ——— IP      6      6 ——— 2<sup>nd</sup> Digit</p> <p style="margin-left: 100px;">1<sup>st</sup> Digit</p>			7		Protected against temporary immersion in water
			8		Protected against continuous immersion in water

**Figure 10 - IP Rating Standards [37]**

IP-68 provides a dust and water tight environment required for the smart tire monitoring system.

## 4.4 Sensor Selection

Research presented in [7] suggested that there exist 3 main types of sensory technologies that can be applicable for measuring strain related information. These sensors are foil based strain gauge sensors, optical based sensors and piezo-electric based PVDF sensors. Each option is summarized through its pros and cons below and a decision matrix is constructed.

### 4.4.1 Strain Gauges

Strain gauges work on the principle of electrical resistivity changes based on physical deformation. The sensor itself is usually a comb like pattern where the output of the sensor is passed through a Wheatstone bridge and amplifier sensory to read out meaningful values. The sensor is attached to the medium by a strong glue or epoxy such as Cyano-Acrylate. Cost is low per sensor (usually \$10 or less). Sensors are very light, and are passive. However since they output very small voltage differentials, it is important to take the necessary precautions to maintain reasonable SNR levels. This often involves placing buffers or signal amplification circuitry at a close proximity to the sensor.

In case of the smart tire system, the very low Young's modulus of the rubber, 0.01-0.1 GPa [41], makes the strain gauge solutions not very suitable. Simply put, the strain gauge based systems are usually rated to a maximum strain of +/- 5% for one time only. For repeated usage, manufacturers advise to stay within strain limits of +/- 0.24% strain. Needless to say, this is well below the expected strain deformation of the tire, where on the sidewall estimations indicate a strain of 5-6% at each revolution.

### 4.4.2 Optical Sensors

Optical sensors come mainly under two categories. One uses CCD based cameras to acquire images to be processed into video streams. For this type of application, the medium under test is usually coated with precisely marked patterns, such as the phase-shifting Moiré patterns [22]. The second application kind involving optics is the laser based fiber Bragg grating methodology [21].

Sadly these options remain to be quite expensive. More so, not enough studies are presented where these sensory technologies are stressed through harsh conditions. Although non-intrusive and light in

weight, care must be taken to realize that it won't be trivial to attach either the cameras or the optical fibers to a rotating car tire and expect reliable operation at all times.

#### 4.4.3 Piezo Based PVDF Sensor

These sensors provide a cheap (less than \$8 per sensor) method to measure strain changes. Sensors are passive and yet are capable enough to drive out meaningful voltages of up to +/- 10V. This is good, because unlike the strain gauges, signal amplification would not be necessary for the piezo sensors.

They are very light in weight and are Mylar coated. By finding a suitable epoxy, they can be directly glued onto the inner surface of a rotating tire. These sensors are often used in traffic sensory related applications and are stress tested for over a few million cycles. They are suitable candidates for the smart tire system lifetime. A few million operational cycles roughly translate to 100 hours of continuous operation at 120 km/h travel speed. Sadly, at this point the sensor manufacturers have not tested these sensors for any longer operational cycles.

#### 4.4.4 Sensor Technologies Comparison Matrix

To follow a thorough methodology to pick the most suitable sensor solution, a decision matrix is constructed for the 3 different sensor technologies as shown in Table 1.

**Table 1 - Smart Tire Sensory Selection Matrix**

Features Sensors	Nominal Strain Measure (<= 5%)	High Strain Measure (>5%)	Price	Sensor Technology (Active/Passive)	Light Weight	Durable	Rank
Strain Gauges	+	-	+	-(Passive but complex amplifier required, [43])	+	-	2 <sup>nd</sup>
Optical Sensors	+(CCD)	+(CCD)	-(CCD)	+(CCD-Passive)	-(CCD)	-(CCD)	3 <sup>rd</sup>
	+(Fiber)	+(Fiber)	-(Fiber)	+(Fiber-Passive)	-(Fiber)	-(Fiber)	4 <sup>th</sup>
PVDF Piezo	+	+	+	+(Passive)	+	+	1 <sup>st</sup>

As summarized in the decision matrix in Table 1, the piezo based PVDF sensor solution was picked to be further used in this project.

#### 4.5 PVDF Sensor

After deciding on PVDF as the sensory solution, Measurement Specialties Inc., a US based sensor manufacturing firm was contacted. They were kind enough to send 3 samples for various sizes of different PVDF sensors. Upon experimental trials and oscilloscope measurements, it was seen that PVDF sensor with model number LDT2-28K with Lead/Rivets was adequate for the project needs. Shown in Figure 11 (not drawn to scale) is the picture of the mentioned sensor. The dimensions are 7cm x 1.6cm. Datasheet of the sensor can also be found in Appendix A.



**Figure 11 - LDT2-28K Piezo-based PVDF Sensor (Measurement Specialties Inc.)**

Shown in Figure 12 is an electrical model of the PVDF sensor, where  $C_f$  is the film capacitance, and  $R_f$  is internal film resistance.

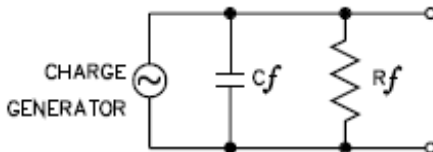


**Figure 12 - PVDF Sensor Electrical Model**



An oscillatory excitation on the sensor made by hand was strong enough to produce voltage swings of +/- 10 volts. At this point it is realized that no additional amplification would be required with these PVDF sensors. However the noise levels of the generated signal were not measured.

The sensors are rated for operations below 90C. Sadly, this might be an issue for long term durability of these sensors in hot summer road conditions as the inside of a tire might get very hot [44].

Operating temperature will also affect the produced PVDF signal quality. This change in behavior can be monitored more closely by implementing a thermistor into the system. However this is not done within the context of this work.

Data acquisition sampling rate formulation derived in Eq. 7 is used to calculate the desired sampling rate for the smart tire application for 40 km/h travel speed. Shown in Table 2 are these estimations.

**Table 2 - Sampling Frequency Calculations for Various Sensing Lengths and Sampling Points for 40 km/h**

<b>Effective Sensing Length (cm)</b>	<b>N<sub>samples</sub> captured within Effective Sensing Length</b>	<b>Sampling Frequency (f<sub>s</sub>) (Hz)</b>
7	3	476
	2	317
	1	159
5	3	667
	2	444
	1	222
2	3	1667
	2	1111
	1	556

If two data samples are to be collected every 5 cm of wheel travel at 40 km/h, then the sampling frequency should be 444 Hz and so on.

#### **4.6 Epoxy / Glue Selection Process**

The reader should keep in mind that finding the suitable epoxy for this project was not a trivial task. Overall the entire process took almost 2.5 months. The problem mainly boiled down to the fact that there doesn't exist too many solutions to provide reliable bonding to automobile tire rubber and the sensor's Mylar coating.

First and foremost, the inside of a tire has a surface coated with numerous chemicals to increase prolonged lifetime. For appropriate bonding, this layer of impurities needs to be cleaned. This can be achieved by either sanding the tire medium or by using a rubber cleaner chemical (primer) with a scraping tool. The latter was kindly donated by the Tech local distributors (Rub-O-Matic Rubber Cleaner) and was used in this project. It is fair to say that using the chemical cleaner along with the scraping tool is much faster and easier than using a traditional sand paper.

Another issue faced throughout the quest for the appropriate epoxy was the fact that even though a few solutions do exist that provides perfect rubber vulcanization; some of these solutions were only sold in US. Apparently some of these fluid patches were also used by military applications and hence their sale to Canada was somewhat problematic. For instance, entry #6 in the Table 3 is a good example. This product is not sold outside of U.S. without special permission. The product is hosted on a website where numerous videos and articles explain the success of the product.

The biggest and by far the most important issue faced during the epoxy selection process was simply the fact that most of the features advertised on product packages and/or websites are extremely biased and often wrong. Twelve different epoxies were tested. Each promised a permanent bonding to rubber either directly stated in product description on the package, or through different marketing mediums like the internet.

Each epoxy was used to first cure a piece of Mylar to tire rubber and the strength of the bonding was tested by hand after curing was fully complete. These tests refer to "Mylar Bonding" and "Rubber Bonding" in Table 3. If results were found promising, then the epoxy was further tested on the PVDF

sensor, named “PVDF Bonding”, just to verify that it did not alter the electrical behavior of the sensor by any means. As a last step, the epoxy and sensor combination applied on a piece of rubber tire specimen was stress tested by a crank-shaft mechanism that excited the rubber specimen such that the tire sidewall deflections were big enough to represent realistic road behavior at each cycle. This test is referred as “Stress Test” in Table 3. Details of the stress testing along with the properties of the crank-shaft mechanism are presented next.

**Table 3 - Epoxy / Glue Testing Summary and Comparison**

	Name	Brand Name	Rubber Bonding	Mylar Bonding	PVDF Bonding	Stress Test (with Sensor)
1	PL Fast Grab Premium	LePage	Not Good	Yes	N/A	N/A
2	Rubber Cement	Victor	Okay	Yes	N/A	N/A
3	Universal Cement	Victor	Not Good	Yes	N/A	N/A
4	Universal Cement	True Flate	Okay	N/A	N/A	N/A
5	Pres-Tite Contact Cement + 3M Foam	LePage	Very Good	Yes	Yes	1 hour
6	Liquid Patch	Safety Seal Plus	Very Good	Yes	Yes	1 hour
7	Flexible Plastic Adhesive	LePage	Okay	N/A	N/A	N/A
8	Amazing Goop Household Flexible Plastic Waterproof Adhesive	Eclectic Products	Very Good	Yes	Yes	1 hour
9	Amazing Goop Household Flexible Plastic Waterproof Adhesive	LePage	Not Good	N/A	N/A	N/A
10	Rubber Cement	SuperCycle	Not Good	N/A	N/A	N/A
11	Chemical Vulcanizing Fluid + Patch	TECH	Good	Okay	Yes	<1 hr
12	Cyano-Acrylate (CC-33A)	KYOWA	Very Good	Very Good	Very Good	Over 10 hrs

As summarized in the Table 3, numerous epoxies were tested. In the end, it was found that the Cyano-Acrylate provided the most reliable bonding to primed rubber. Amazing Goop also turned out to be quite an effective product. It not only is sold commercially at hardware stores, but also has provided a much better flexible bonding than some of the other solutions that are sold exclusively to the tire companies through private distributors.

The prolonged stress tests showed that the Cyano-Acrylate solution by itself wasn’t enough. Simply put, the bonding is so strong that it eventually caused physical damage to the sensor itself. An inventive solution had to be developed and is detailed in the next subsection.

#### 4.6.1 Sensor-Epoxy Durability Testing & Verification

In order to verify the durability of the sensor-epoxy pair, a simple mechanism had to be built for testing purposes.

Pictured in Figure 13 is the crank-shaft mechanism used to stress test the sensor samples. This mechanism was put together by Jennifer Bastiaan.

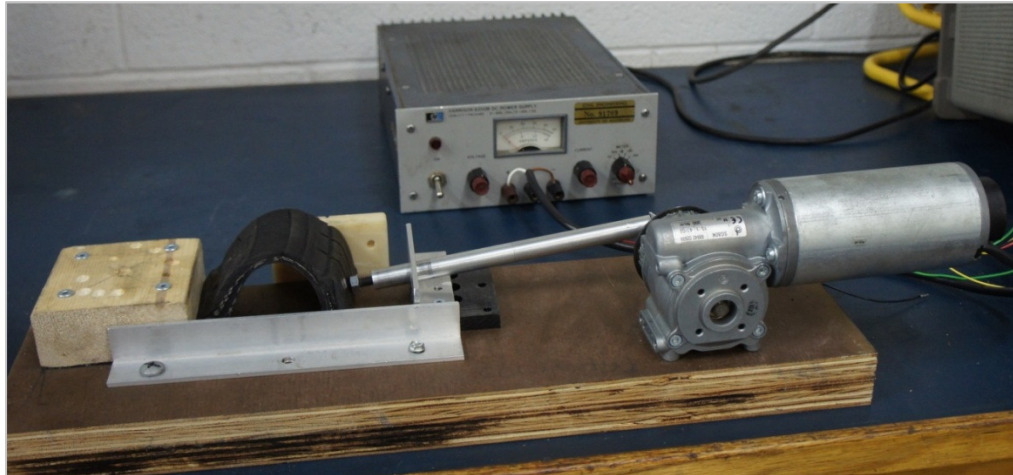


**Figure 13 - Crank-shaft Mechanism for Sensor and Epoxy Durability Testing**

FEA analysis performed by Jennifer Bastiaan [38] suggested that the worst strain deformations are to be expected on the sidewalls of the tire. Simulating the FEA model for a medium size car indicated that in worst case, which happens to be during hard braking, the lateral deformation of the sidewall would be around 17 mm. In order to stimulate such a contour, a longitudinal oscillatory displacement of 40 mm is applied to the tire specimen through the crank shaft mechanism. Also to simulate driving speeds of 30 km/h, the system was run at 4 Hz frequency. The signals coming from the sensors were analyzed through an oscilloscope. Scope waveform captures were repeated in timely manner to observe the decaying effects on the signal strength as well as SNR quality over time.

Though quite crude, this mechanism provided great insights into the long term durability of the sensor-epoxy pair. Simply put, the sensor worked fine and it kept on converting mechanical strain to electrical signals of enough strength to drive the inputs of a DAQ system. The epoxy solution also

worked fine, the sensor was fully attached to the tire specimen at all times. This bond was not damaged even though the tire specimen was subjected to the worst case strain values.

At this point something interesting happened. It was found that after a few hours of operation, there was a significant reduction in peak-to-peak signal readings coming from the sensor. First this was thought to be an effect of the epoxy (i.e. something kept curing over time), then it was thought maybe it is somehow related to the sensor material properties itself. The latter got resolved by speaking to an application specialist from the sensor vendor company. It was mentioned that this type of PVDF sensors are used heavily in traffic applications where stress tests typically included at least a few million cycles.

After careful observation of the tire and sensors specimens after the tests, it was found that all the signal degradation of the system under test was related to minor physical and mechanical problems.

One problem found was that the bonding of the Cyano-Acrylate was so strong that it caused the sensor to buckle at various parts. Shown in Figure 14 is the PVDF sensor after a few hours of stress testing. The buckling is thought to be the main reason for signal degradation.

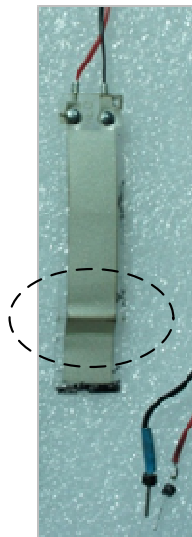


**Figure 14 - PVDF Sensor Buckling Issue**

First this issue was tried to be fixed by applying two different epoxies in conjunction. The tip of the sensor where higher strain levels are expected, the flexible fluid based Amazing Goop was applied. However by itself, this solution was not enough.

Second, it was suggested by author's supervisor to impose a mechanical constraint to let the tip of the sensor move freely. This was implemented simply by placing a piece of paper-clip at the tip of the sensor. In this set up, Cyano-Acrylate is applied to the sensor; however the part below the paper clip is not glued anymore and is left to swing freely. This took care of the buckling problem.

Interestingly enough, this by itself was not enough to solve the SNR issues. It was seen that after a few hours of operation the signals were still getting noisier and patterns were not consistent. After careful observation, it was seen that the Mylar coating of the PVDF actually caused a dent in the tire specimen, and hence after a while the motion of the entire sensor and tire patch was deformed and got affected. Pictured in Figure 15 is this phenomenon.



**Figure 15 - PVDF Sensor Creating a Dent into the Rubber Specimen**

At this point another practical solution was added into the system. This was simply gluing a small piece of plastic right under the tip of the PVDF sensor. This piece of plastic provided a smaller friction coefficient and hence the PVDF started freely moving back and forth without causing a dent into the tire anymore. Shown in Figure 16 is the fully modified version of the sensory system.

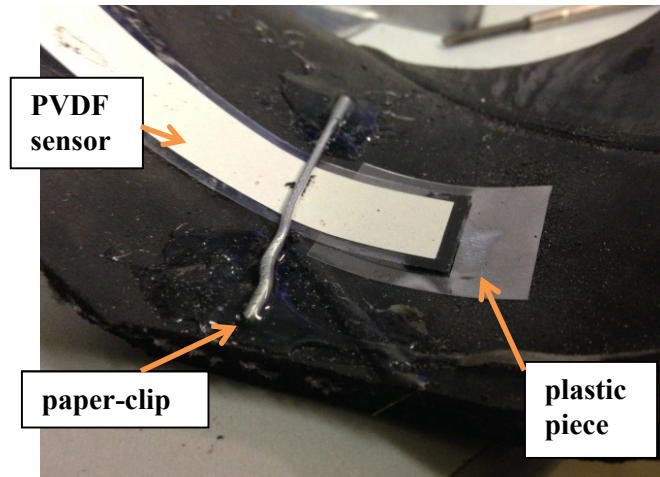


**Figure 16 - PVDF Sensor Mechanical Practical Solution**

This system was then stress tested rigorously through over-night tests. It was seen that the peak to peak voltage values remained within reasonable range, and signal waveform patterns reflected a proper sinusoidal function at 4 Hz. Shown in Figure 17 is the output of the sensor for the 4 Hz oscillatory crank shaft input.

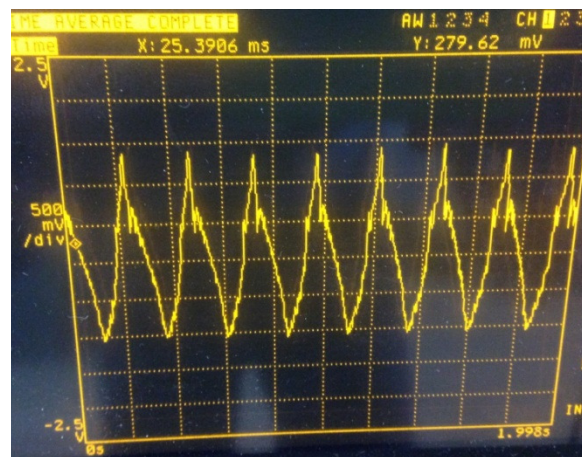


**Figure 17 - Oscilloscope Readings of the Modified Sensory Setup**

While the signal did manage to remain within reasonable values, a %10-%15 amplitude degradation was observed in the created PVDF voltage for extended operations over 3 hours. Once fatigued enough, the sensor always gave out reduced readings and hence the effect is not reversible. This issue, although not crucial for the scope of this thesis, should be kept in mind if PVDF sensors are to be implemented in smart tires someday.

At this point it was concluded that the designed solution was durable and functional enough to be implemented inside a tire. The first sample of the smart tire was then born with 6 PVDF sensors implemented, through the technique described above. Shown in Figure 18 is the picture of the smart tire. The sensors were implemented into the tire by Jennifer Bastiaan.



**Figure 18 - Fully Assembled Smart Tire Monitoring System**



## **4.7 Electronics Selection**

### **4.7.1 Analog to Digital Converter (ADC) Selection**

The electrical properties of the signal emanating from the PVDF sensor was analyzed and it was seen that a voltage swing of +/- 2.1V is produced when the sensor is bent back and forth in an amount of deflection that it would face during real driving conditions.

Hence the aim became to find a suitable ADC chip to do reliable data acquisitions. The sought after chip should have at least 6 channel inputs where differential inputs are desirable, however not mandatory.

Upon discussing the needs with a Linear Technology Field Application Representative, it was mentioned the ADC LTC1859 is suitable for this task, and it already comes populated on a demo board with 8 inputs for a very reasonable price (<\$50). The chip is capable of converting 8 channels and provides a cumulative throughput of 100 kSps and is 14-bit in resolution. The converted signals' readings are then sent out to a processor through the SPI bus.

One benefit of using this particular approach was the fact that Linear Technology already provided numerous demo tools and examples to be used with the ADC. This not only made the testing phase run a lot smoother, but also helped us make a really nice, fully operational, project demo for the project funders' (General Motors) quarterly meeting.

### **4.7.2 Microprocessor Selection**

Reader should keep in mind that this subsection refers to not only the selection of the microprocessor itself, but also aims to find a fully assembled hardware development platform ready for use. For this aspect, the overall cost of the system, Integrated Development Environment (IDE) availability, technical support and online resources were taken as the main criteria.

At this point the author should mention that there exists numerous microprocessor based development board solutions that would be perfectly suitable for this project. Numerous vendors release multiple families of development boards. Most priced well within hobby circuitry range (<\$500), embedded electronics of our current age offers an amazing playground for those with a thirsty mind in digital

design. For the price of a fancy toy, these electronic development boards are great mediums to learn and apply digital design skills.

For this project, the Arduino development platform was selected. This platform was chosen because it already offers an immense amount of resources online both through wiki-style pages and forums. It also is priced very reasonably (<\$100). Arduino platform is also very versatile as due to its vast popularity there exists numerous additional electronics, named “expansion cards” that can be populated on the Arduino development board. By doing so the functionality of the board can be enriched; such as adding an Ethernet connection or a SD card reader.

Two different flavors of Arduino development boards were tested. These are Arduino UNO, and Arduino MEGA ADK.

Shown in Figure 19 are pictures of both Arduino development boards. The details of the platforms along with the electronics datasheets can be found on Arduino’s website ([www.arduino.cc](http://www.arduino.cc)).

Schematic of the entire monitoring system can be found in Appendix C.

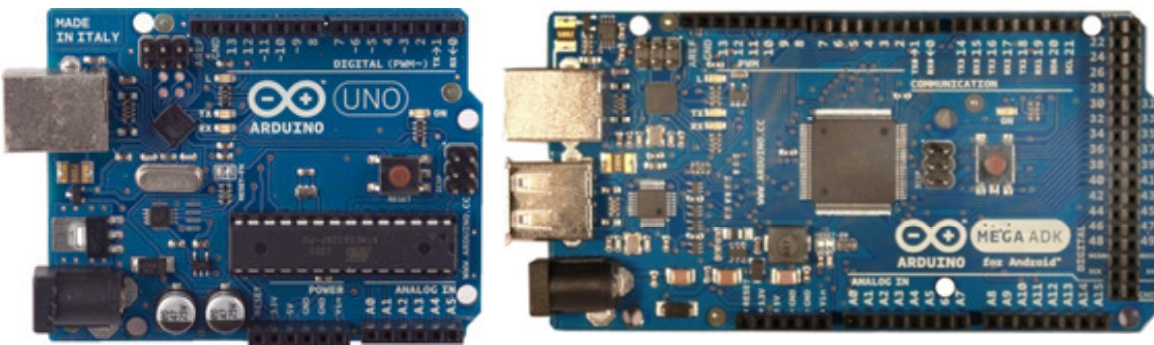


**Figure 19 - Arduino UNO and Arduino MEGA ADK Development Platforms**

### 4.7.3 Mobile Data Storage Options

As mentioned in the previous subsection, Arduino boards can interface with an SD card once the proper expansion module is installed. For this application the expansion card “RTC Data Logger” from Adafruit was chosen. This expansion board enables data to be written and read from an SD card. Shown next in Figure 20 is the mentioned expansion card.

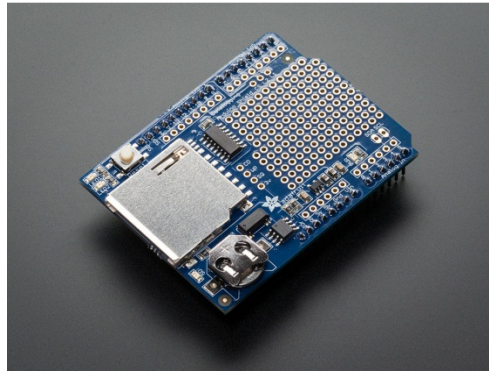


**Figure 20 - Adafruit SD Shield Expansion Card**

Unlike the UNO, Arduino MEGA ADK development board comes equipped with a Type-A USB plug. The board also provides USB driver files and can be configured to act as a USB host. By doing so, the incoming data streams can be recorded onto a USB stick as well. However, it was found the hard way that coding a USB driver to work reliably with the USB stick was not a trivial task and is not recommended for the weak hearted. Shown in Figure 21 is the Arduino MEGA ADK board with the attached USB stick for data storage.

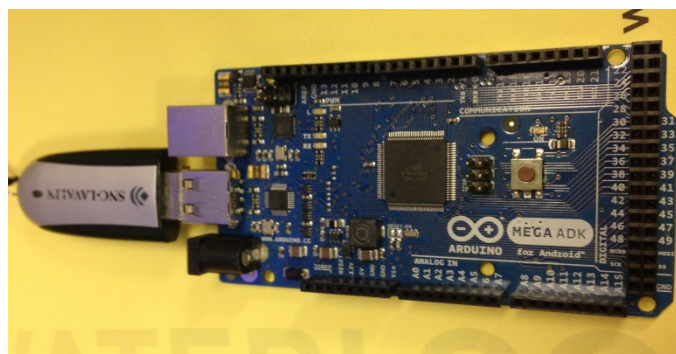


**Figure 21 - Arduino MEGA ADK with USB Stick for Data Storage**

## 4.8 Battery Power System Design

One key feature of the smart tire monitoring system was the standalone operation. This essentially implies that all the electronic components of the system should be supplied power through a battery. This battery should also be charged from the same USB line that the host PC communicates with the microcontroller.

Oddly enough, none of the battery packs available for Arduino platforms deliver this functionality. They fall short in mainly one key aspect. They all house a mechanical switch that puts the battery pack either in “charging” state or “supply” state. As the name implies, in the “supply” state, the battery is feeding current into the circuit. The battery packs have only one type-B mini USB plug. For this project, both charging and microcontroller-PC communication needs to be done through the same USB cable. Sadly, this functionality is not readily available in the battery packs available on the Arduino market place.

For this project, the Lithium Backpack battery solution from Liquidware was purchased [45]. This pack is capable of providing 2200 mAh at 5V DC and is designed specifically for Arduino usage.

It is helpful to represent the current needs and lacks of a battery system at this point. Shown next in Figure 22 is a simple diagram showing the operational behavior of the battery pack.

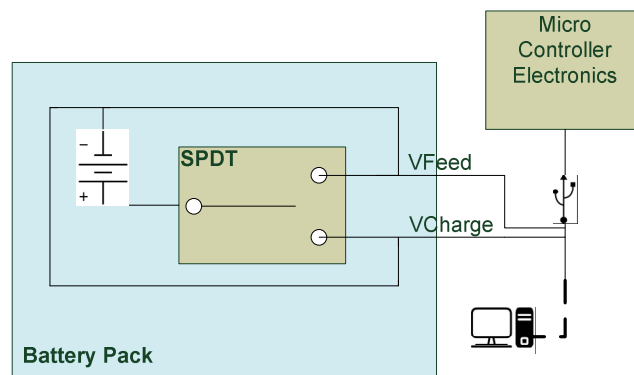


**Figure 22 - Arduino Battery Pack Functional Block Diagram**

As summarized in Figure 22, the battery module lacks the sought after functionality for two main issues. First issue is that the battery module needs to be put in an either charging or feeding mode through a SPDT mechanical switch. Second issue is the fact that the battery pack only has one USB connection. If the battery pack is to be charged, the USB cable should be connected to a power source, but when the battery pack is in feed mode, the USB cable should be connected to the device to be powered. When PC communication is desired, the same USB cable should then be connected to the PC. All these issues make the practicality of standalone system operation very cumbersome and hard to be dealt with.

What happens next is again quite un-orthodox in terms of scientific methodology but yet has succeeded to solve the problem.

External USB hard-drives are used very commonly these days and they offer to provide easy means of abundant storage space upon need. Some of these USB based hard-disks actually have mechanical disks spinning in them. Needless to say this does require a significant amount of power where a single USB port fails to provide as they are capped at 5mA.

A split USB cable is used in applications where more current is needed for USB device operations such as in the case of USB hard drives. The cable has 2 USB plugs on one end, and 1 in the other. The device is connected to the PC through two USB ports and can provide the 3<sup>rd</sup> USB plug data communication with the PC as well as two times more current supply. Without this little trick, most of the USB hard-disks would not have enough power to operate and would require a separate power supply which might make mobility an issue.

An empty USB hard drive enclosure was purchased from a local computer store and the split USB cable that came with it was adopted for this project. More so, the mechanical switch of the battery pack was hacked by removing the mechanical switch completely and by adding wire extensions to the switch leads. This leads were then soldered on to the terminals of the main power switch placed on the enclosure box. Tricky as it may sound, these tiny modifications gave the smart tire monitoring system the following capabilities:

- System now runs fully in standalone mode through the battery fed power
- System is controlled reliably through a power switch (ON/OFF)

- When system is connected to a host PC, and the switch is in OFF mode, the battery automatically goes in charging mode and charges itself through the PC's USB port while the PC also does data communication with the microprocessor through Arduino IDE

It should be noted at this point that out of all the capabilities mentioned above, especially the third one needs more attention. Interestingly enough, this type of functionality has never been offered to Arduino development systems before and even the off the shelf solutions offered in the market do not seem to have this functionality. For using the battery pack in conjunction with the Arduino development board in this specific method, the approach presented in this project is novel.

#### 4.9 Arduino DAQ Performance

As pointed out by the algorithm flowchart in Section 4.2, the software design of the DAQ system was not very complex. The system is simply asked to record the incoming data on to a storage medium (SD Card for Arduino UNO, USB Stick for Arduino MEGA ADK). Once the designs were functional the performance of these systems were benchmarked against an industry off the shelf DAQ system from National Instruments (NI-USB 6210), which is a 16 input, 250 kSps DAQ device.

It should be mentioned that the software and firmware design of this approach turned out to be way more complex than ever thought. As Table 4 suggests the performance of both Arduino systems were noticeably low when the system is asked to record the incoming data streams onto a storage medium. This misbehavior occurred mainly of two reasons.

**Table 4 - Arduino-based DAQ Performance Comparison and Evaluation**

Platform	External Storage	1-Channel Data Acquisition Rate	6-Channels Data Acquisition Rate	Comments
Arduino UNO	SD Card	1.2 kHz	800 Hz (per ch.)	Hardware limitations. Further study is not necessary
Arduino MEGA ADK	SD Card	1.6 kHz	1.1 kHz (per ch.)	Hardware has higher capabilities. Further studies can be done to fully utilize the board capabilities.
	USB Stick	1.8 kHz	1.3 kHz (per ch.)	

First reason is due to the fact that the ADC was converting each signal acquisition into a word-type data structure that consists of 4 Bytes. Sadly Arduino boards have very limited program RAMs (usually a few kB's) and hence this memory gets full very rapidly unless a very smooth data pipelining is to be implemented, which is also not possible due to the reason outlined below.

Second reason for functional misbehavior was due to the fact that microprocessors are not very accurate in execution times and they are not fully suitable for application where multi-tasking is needed. Microprocessors are sequential elements. Each line of code is executed sequentially. Sadly, the microprocessor cannot guarantee the time duration of each line. In our application, it was found that the performance of DAQ varied (however tiny) per each test run. This was truly heart breaking, mostly because these functional deficits were never mentioned in product datasheets. Upon further research into this topic, it was found that most of the hobby electronics simply deviate from microprocessors to more powerful systems such as FPGA's in order to achieve better data pipelining and faster processing speeds.

At this point it was concluded that simply using a microprocessor by itself would not be sufficient for harvesting the required data for smart tire application since the desired data capture rate is higher than that of Arduino's performance capabilities.

It should also be mentioned here that the above mentioned two Arduino based data acquisition systems are in fact full operational DAQ systems. Although low in sampling rates (less than 2 kHz per channel), these solutions are comparable to solutions offered in the market for purchase over \$300. In fact, the solution developed on the Arduino UNO for recording a single channel for 1.2 kHz on SD card beats the currently available market solution.

#### 4.10 Off-Shelf DAQ Selection

In a way all the electronics and the design itself did work. However once executed together, the components fell short of their promised data throughput. It was disappointing to read out only 1 kHz sampled packages even though the ADC was rated at 100 kSpS which is equivalent to 100 kHz sampling in theory.

Since the primary purpose of this project was to collect data from a smart tire, developed at the same time by the other team member Jennifer Bastiaan [38], there was a tight time constraint on the DAQ design and implementation. To do so, industrial stand-alone DAQ solutions were evaluated, and a suitable one was picked to provide the necessary data for the project. The requirements were simple; the DAQ had to be portable, support standalone operation, is capable of capturing at least 6 channels simultaneously, and can do data recording on SD Card. Three candidates promising this type of functionality are evaluated and are summarized in Table 5.

**Table 5 - Off-shelf DAQ Comparison and Evaluation**

<b>Vendor</b>	<b>Model #</b>	<b>Input Ch.</b>	<b>Sampling Rate</b>	<b>Size</b>	<b>Storage</b>	<b>Battery Operation</b>	<b>Price (\$)</b>	<b>Availability</b>
<b><i>DataQ Instruments</i></b>	DI-710	16 SE 8 Diff.	14 kHz	Fits	SD Card	Yes	600	Immediate
<b><i>National Instruments</i></b>	9215+ 9191	4 Diff.	100 kHz (per channel)	Too big	On board (4GB)	Yes	1000	Immediate
	9220+ 9191	16 Diff.	100 kHz (per channel)	Too big	On board (4GB)	Yes	2300	Immediate
<b><i>Techmatron Inc.</i></b>	LGR-5325	16 Diff.	100 kHz	Too big	SD Card	Yes	1650	Immediate



Due to price and ready availability, the DI-710 from DataQ Instruments was picked and retro-fitted inside the smart tire monitoring mechanical enclosure. The device was set to run in standalone mode and the incoming 6 channels were captured on to the SD card at 2.1 kHz sampling frequency per channel.

A non-spillable 12 VDC battery was also added to power the DAQ device since the previously designed Arduino based battery system was no longer applicable. Shown in Figure 23 is the retro-fitted DAQ in the monitoring enclosure.



**Figure 23 - Smart Tire Monitoring System with DI-710 DAQ**

## 4.11 Signal Conditioning Circuitry

Before starting the road tests, it was realized that the high impedance of the PVDF sensor (1M Ohm) was causing issues with the signal readings of the particular DAQ solution. It should be noted that these issues did not arise in the earlier tests with the Arduino electronics. As it turns out, DataQ decided to design a DAQ with lower impedance ratings than most other vendors. This impedance mismatch resulted in cross-talk between successive data channels at high sampling rates. To overcome, a buffer circuitry had to be designed and implemented as shown in Figure 24.

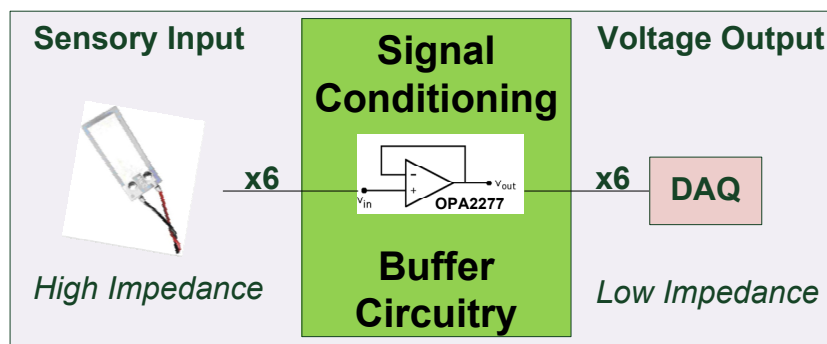


**Figure 24 - Smart Tire PVDF Sensor Buffer and Signal Conditioning Block Diagram**

Fast response, high-precision op-amp OPA2277 (Appendix B) from Texas Instruments was selected for this application. The circuit was implemented on a blank PCB breadboard, and the bench tests confirmed the proper functionality with the attached PVDF sensors. The buffer circuitry successfully diminished effects of the cross talk at the DAQ.

At this point it was believed that the smart tire monitoring system was finally ready for a real road test. The results of the numerous road tests are described in the next chapter.

## **Chapter 5**

### **Experimental Analysis**

So far numerous design issues and solutions to overcome them have been introduced in the earlier chapters. The smart tire was installed on the left front tire of the Chevrolet Equinox EV. Right front wheel of this car was also equipped with a wheel sensor. The wheel sensor was used to collect tire forces for system calibration and artificial neural network training. Shown in Figure 25 is the smart tire fully installed on the vehicle.



**Figure 25 - Fully Assembled Smart Tire Monitoring System Installed on Chevrolet Equinox EV**

Once the tire was fully installed, the car was taken out for a test ride. Details of the road testing are described in the following section.

#### **5.1 Road Testing & Experimentation**

In order to faithfully observe the characteristics of the tire model, numerous tests had to be performed and corresponding data were captured through the monitoring system.

12 different tests scenarios were developed. These scenarios are quite common in vehicle dynamics research and bear no relation to the presence of a smart tire at all. Summarized in Table 6 are the different scenarios used for road testing. These scenarios were compiled by Jennifer Bastiaan [38].

**Table 6 - Smart Tire Road Test Descriptions**

<b>Scenario #</b>	<b>Test Description</b>
1	Light acceleration (from 10km/h to 40km/h)
2	Moderate acceleration (from 10km/h to 40km/h)
3	Hard acceleration (from 10km/h to 40km/h)
4	Very Light Braking (from 10km/h to 40km/h)
5	135° step steer left at 30km/h
6	135° step steer right at 30km/h
7	180° steer left at 30km/h, steering while braking
8	180° steer left at 30km/h, straight braking
9	180° steer right at 30km/h, steering while braking
10	180° steer right at 30km/h, straight braking
11	Sine steer at 30km/h
12	Ring road travel, 40km/h, CW dir., dur=15 min.
13	Ring road travel, 40km/h, CCW dir., dur=15 min.

All the tests mentioned above were performed by Kevin Cochran of Mechatronic Vehicle Systems Laboratory. Tests took place at the University of Waterloo’s ring road, and parking lots.

Once the tests were over, the captured waveforms on the SD card were extracted from the DAQ. As mentioned earlier the car is equipped with a load sensor in its front wheel. On board DAQ system through the dSpace Control Desk captured the data signals from the load wheels as the road tests took place. Once over, both data streams, one from smart tire monitoring system DAQ and the other from the wheel sensor data readings recorded on dSpace were cross referenced and neural network trainings were performed.

### 5.1.1 Road Data Collection

Road tests were carried for all the different scenarios listed in Table 6. It should be noted that the entire course of 13 tests were repeated numerous times. It was the utmost desire to collect as much data as possible since neural network training reliability is directly proportional to the amount of collected data.

Shown in Figure 26 are a few waveforms captured during the tests. Some preliminary calculations and derivations are also shown in the following subsection. It should be noted that the scope of this thesis was to come up with the data acquisition system. Once the data was successfully and reliably collected, there was not much to do within the context of this work. Figure 26 is a snapshot of waveform captures for test scenario #2 mentioned in Table 6. Needless to say, these waveforms do not mean much by themselves.

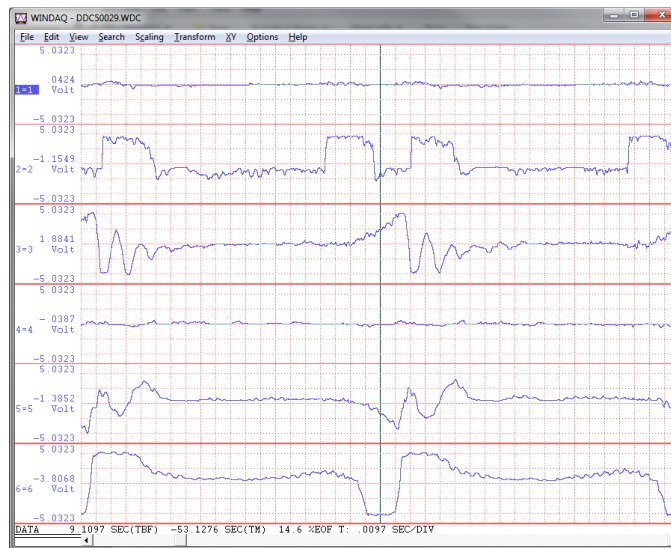


**Figure 26 - Waveform Capture Sample Obtained by DI-710 DAQ**

Therefore reader should refer to Jennifer Bastiaan's PhD. thesis [38] to understand the true meaning and importance of the collected data and how well they can be correlated to vehicle dynamics parameters such as lateral force, normal force etc.

The experimental runs were completed successfully. The smart tire monitoring system managed to capture data from 6 PVDF sensors and record them on an SD card at an acquisition throughput of 11 kHz, which is equivalent to roughly 2 kHz sampling per each sensor channel.

At this point, without the introduction of the new FEA tire model itself, the obtained waveforms are not of too much use quantitatively. However, the collected data for the tire surface already follows the trends of tire strain behavior presented in literature review. Though crude, this was a good indication to confirm the functionality of the system by simple visual inspection of the waveform samples.

WINDAQ SD Viewer software, provided by the DATAQ Data Acquisition System has a few handy features that got utilized for this project. The free software not only reads and displays the captured waveforms from an SD card, but also exports the collected data into an Excel spreadsheet file that can be further processed in other software packages. For this project, Matlab was used for signal analysis and post-processing.

Discrete Fourier Transformations (DFT) converts the collected data samples into list of frequency component coefficients, which essentially is the spectral structure of the raw signal. By looking at the spectral features, effect of each signal frequency can be understood. DFT transforms time-based captured data to frequency-based data. Matlab was used to compute the Fourier Transformations of the collected raw signal. Shown in Figure 27 below is the DFT of the waveform captured during the epoxy-sensor verification test. During this test the crank shaft mechanism, Figure 13, excited the tire sample patch at a rate of 4Hz.

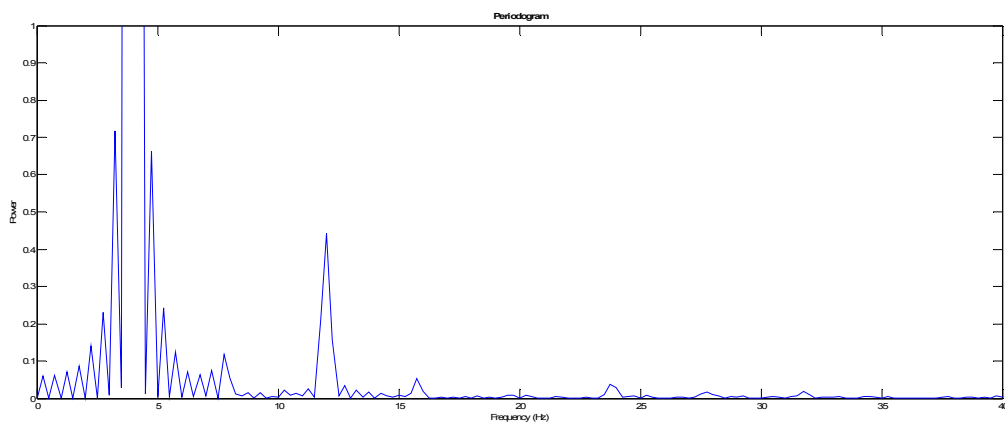


**Figure 27 - Signal Spectrum Analysis of PVDF Collected Data of 4Hz Excitation**

It was also seen that the collected data was prone to noise. A simple filter in Matlab was implemented to suppress the unwanted noise harmonics of 35 Hz and above.

## 5.2 Filter Implementation in Matlab

Since the collected data seemed to be noise prone in an oscillatory fashion, a digital filter was implemented on Matlab and was applied during post-processing phase of the collected data. The purpose of the filter implementation was to smooth out the noisy signal readings at unwanted frequencies. To do so, a two-step process was followed as described in Figure 28.

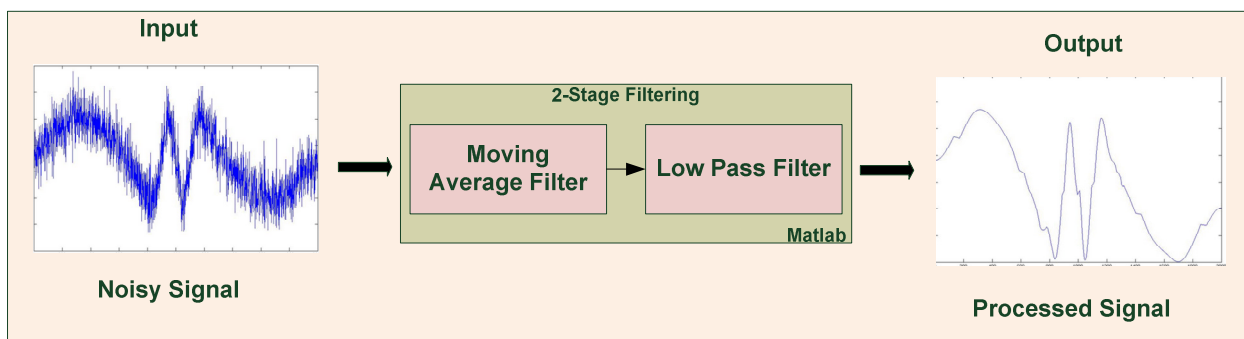


**Figure 28 - Signal Filtering Block Diagram**

First, a moving average filter was implemented. This is to smooth out noisy oscillations at high frequencies. Then a simple low pass filter with a cutoff frequency at 35 Hz was implemented. Aim of this filter to rule out all the unwanted noise emanating from frequencies above 35 Hz that are due to vehicle vibrations. This value was computed by J. Bastiaan through her FEA modal analysis [38]. Matlab's built-in filter command was used to implement both of these filters. A 2<sup>nd</sup> order Butterworth low-pass filter was chosen due to its simplicity.

Shown in Figure 29 is a sample test waveform captured during crank-shaft testing and the corresponding output signal after filtering took place. As can be seen, the filtered waveform had less vibratory harmonics and can deliver a more reliable description of the physical behavior of the system.

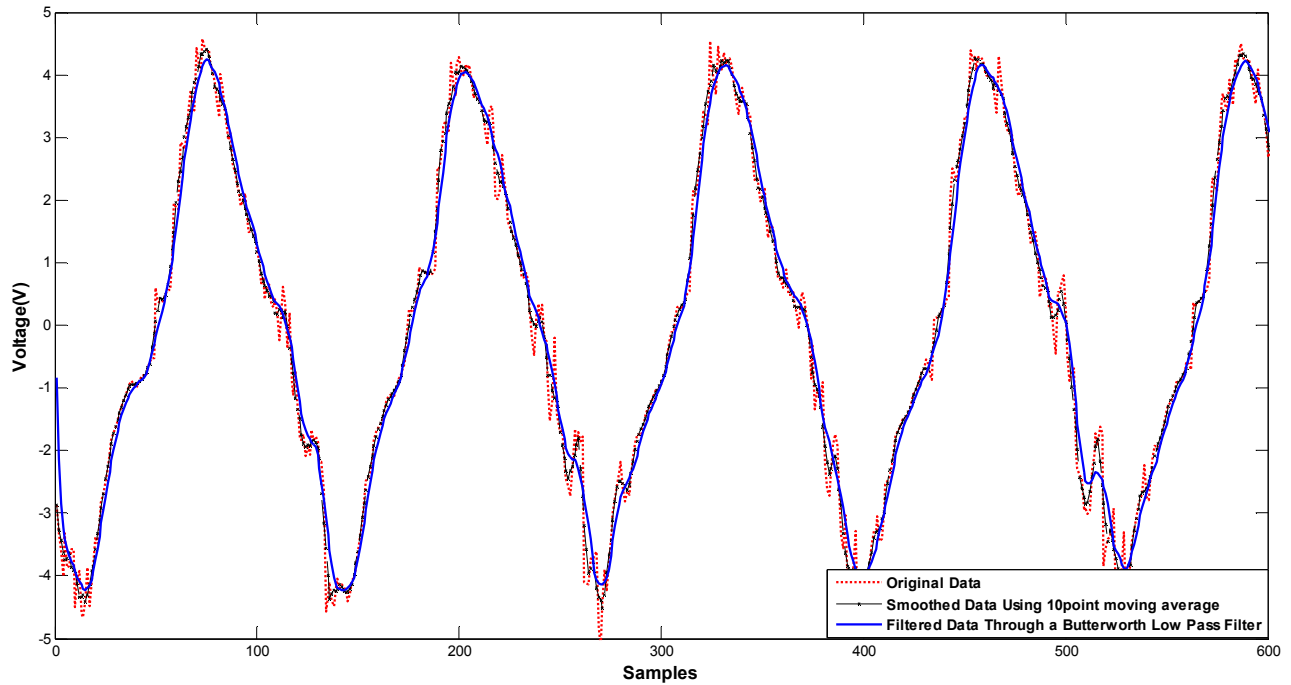


**Figure 29 – Signal Filtering Results**

### 5.3 Post Processing of Collected Data

In order to make something meaningful out of the collected streams of data, an artificial neural network was designed in order to map the behavior of the PVDF sensory reads to that of load wheels readings.

#### 5.3.1 Artificial Neural Network Design & Implementation

ANN's essentially try to mimic the behavior of the human brain to solve engineering related problems [36]. Unlike computational electronics where things tend to take place in a linear sequence, ANN's process the problem by subdividing the work into numerous neurons which is very similar to the way human brain works.

All events might take place in an infinite amount of different possible ways, but the summation of the cumulative probabilities will always be equal to 1, that is the event will take place. By weighing the probabilities between, one can say that there is a 99.99% chance that the event will unfold in a certain way.



ANN's try to observe a similar relationship between data input-outputs by first creating a set of neurons and interconnecting them through arbitrarily assigned probability weights. Then during the network training phase, these coefficients are altered to fit the input-output correlations.

Figure 30 is a high-level block diagram of the ANN designed for the smart tire data analysis. Realize that the vehicle used for testing was equipped with a load wheel sensor, and the normal force ( $F_z$ ) readings of this sensor were fed to the neural network as the output, whereas the 6 PVDF sensors were fed to the network as the inputs.

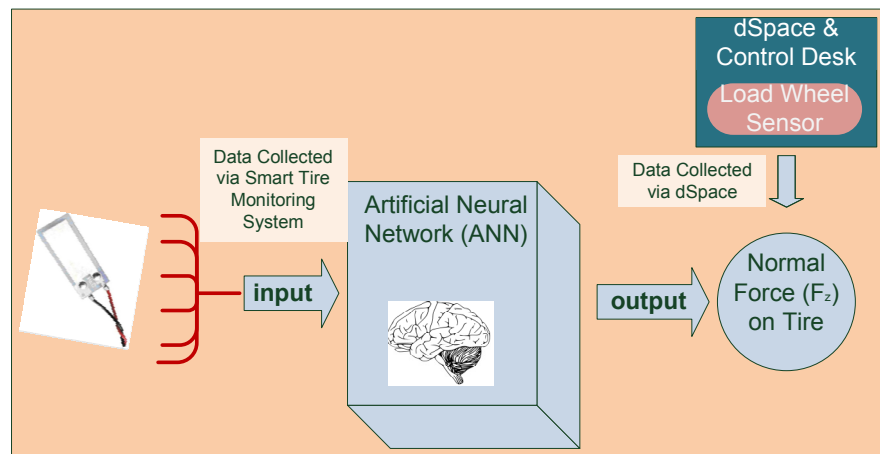


**Figure 30 - ANN Implementation High Level Block Diagram**

The sensor readings coming from each tire form a 6xn dataset. These are the inputs to the neural network. The output of the neural network is a 1xn dataset with normal force ( $F_z$ ) values for left front tire.

Shown in Figure 31 is the graph of normal force readings from the tire load wheel sensor. It should be noted here that the dSpace system used in the testing is only able to capture data for 15 seconds at a sampling rate of 200 Hz.

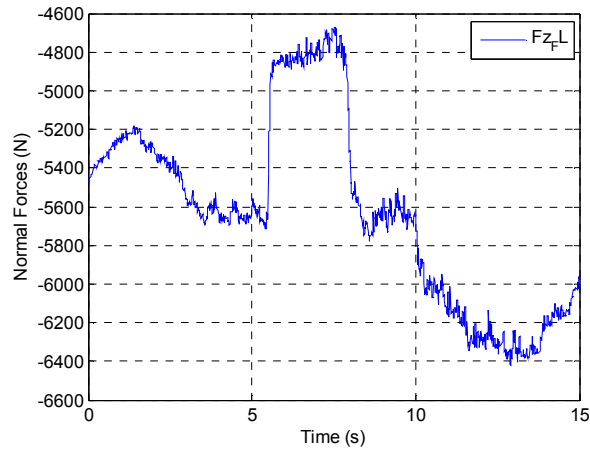


**Figure 31 - Sample Data from Load Wheel Sensor Collected by dSpace Platform**

70% of the dataset was used to train the neural network. 15% was used for validation, and the remaining 15% was used for testing.

Matlab's built-in neural network (nntool) toolbox was used. Few different cases with varying hidden layer counts were tested and evaluated. However in order to get the networks properly trained, the sensor captured data had to be down sampled to 200 Hz. This was necessary since Matlab's toolbox only accepts input and output datasets of the same size.

As a second approach, the dSpace collected data was up-sampled to 2 kHz. Results of these ANNs aren't shown as the performance did not increase.

It should be noted that the ANN based analysis presented above is very preliminary and should only be accepted as a proof-of-concept solution for utilizing multiple PVDF based sensors for smart tire monitoring. Further studies on this topic are to be published in Jennifer Bastiaan's PhD. thesis [38].

**Table 7 - ANN Performance Comparison & Evaluation**

	Neural Network Topology	Performance			Performance Graph	
1		Target Value	MSE	R		
		Tra.	2101	493.68		0.99996
		Val.	450	477.94		0.99901
		Test	450	625.37		0.99871
2		Target Value	MSE	R		
		Tra.	2101	497.3		0.99899
		Val.	450	445.36		0.99894
		Test	450	571.82		0.99884
3		Target Value	MSE	R		
		Tra.	2101	487.58		0.99899
		Val.	450	590.04		0.99894
		Test	450	626.62		0.99884
4		Target Value	MSE	R		
		Tra.	2101	480.71		0.99899
		Val.	450	446.26		0.99059
		Test	450	511.25		0.99889

Mean Squared Error (MSE) is the average squared difference between target values and the actual outputs. Lower the value, better the performance of the ANN. Regression value (R) measures the correlation between the real outputs and the target values. 1 represents a close relationship, whereas 0 means relationship is random.

As can be inferred from Table 7, although crude, ANN did manage to find a correlation value greater than zero. Test case #4 in particular had the best overall performance with lowest MSE for testing data.

#### **5.4 Arduino Based Data Acquisition Results**

Design of the data acquisition systems on Arduino platform did not make it to the road tests due to reliability issues. However each system did work reliably if the sampling rates were kept as low as 1 to 1.5 kHz. These frequencies are of course not enough for operation at high driving speeds, but it should be noted that the functionality of these in-house developed systems are, aside from sampling rate, on a par with industry leaders' marketed products.

Two things were realized while the tests were being performed on Arduino systems.

- Microprocessor based systems are not reliable in terms of execution timing

This issue was noticed by careful tracking of processor counter within the Arduino platform. Arduino's built in *millis()* function returns the number of milliseconds since program execution. Used efficiently, this function is a great tool for analyzing timing behavior within the microprocessor.

It was seen that there were abnormal time gaps in between executions. However these gaps were happening in a random like fashion. This eventually lead to system halts and crashes once in a while. Hence, as described in Table 4, the throughput of the data acquisition systems were always stuck at low values, even though the ADC is running at 100 times faster speeds.

A simple reset solved most of these issues related to system halts and crashes; however it was quite annoying to see that the Arduino systems were not fully reliable for continued operation.

- Writing data to SD card is not a straight forward process

Numerous issues were faced when data interfacing with the SD card. Firstly, Arduino only works with Fat16 or Fat32 formatted SD cards. This limits the storage size to 2GB. While this storage is plentiful for the smart tire application, it still is quite strange why SD cards of bigger size are not supported by the Arduino platforms.

Another interesting behavior was observed while analyzing the simultaneous write speeds to the SD card. It was seen that once every 45 write cycles or so, the system happens to halt for a few milliseconds, and then restores its original speed. This phenomenon was in fact the main reason why the Arduino based DAQ was not functionally reliable. Further tinkering with this behavior lead to something very interesting.

The SD card write behavior was tested for different write speeds. In each iteration the delay amount in between successive writes were altered. The performance of the system was observed and evaluated by analyzing the readings of the processor clock. By adding an external counter to count the number of write cycles, and asking the system to go in a circular buffer mode every 44 cycles did improve the writing performance.

It should again be noted that time was scarce while these little revelations were taking place. Author had to move on to road experimentation on a timely manner. Author believes that the tricky behavior of SD card should be further analyzed especially on low cost microprocessor based systems. For any application with sampling rates above 1 kHz this behavior needs to be fully understood for reliable operation.

## Chapter 6

### Concluding Remarks

#### 6.1 Summary

A smart tire monitoring system was designed and implemented. PVDF based piezo electric sensors were embedded inside rubber tire to measure strain related data. This data is collected in order to estimate various important parameters regarding the tire such as forces and moments acting upon it, coefficient of friction and inflation pressure. The sensor embedding and attachment procedure is novel and was developed specifically for this application.

System electronics were implemented inside a robust IP-68 rated enclosure. This enclosure was mounted on a car wheel and successfully recorded data during normal driving onto an SD card.

Data collected from the PVDF sensors were post-processed in Matlab for a two-stage filtering. An ANN was also built to correlate the sensor data to the wheel normal force ( $F_z$ ) readings given by an industry grade load wheel. Having such a device was really fortunate and made the neural network training process very straightforward. Although the correlations were very crude, this study shows a promising way to analyze the strain related information from car tires by using PVDF sensors in conjunction with ANNs.

Arduino-PC data communication and simultaneous battery charging was achieved by utilizing a split type hard drive cable. This solution is also novel and still is not offered by any product sold within the Arduino community.

Two low cost data acquisition systems were designed in-house with the Arduino platforms. These systems cost very reasonable (under \$100) and are equivalent to that of market sold products for over \$250. This is a price reduction of 2.5.

It was seen that using microprocessors for time critical applications is not a good choice if parallelism within the software is needed. In other words, microprocessors are better for applications where the executions can be done sequentially.

## **6.2 Future Works**

For future work, better electronics platforms can be analyzed to be implemented in the smart tire monitoring system. A great candidate is using a low cost FPGA to handle the computations and SD card writes. By doing so, the ADC's true power and capabilities can be fully utilized.

Also, further techniques can be studied to broadcast the collected sensory information in real-time to the CAN network. This information can then be implemented as an input to be used for vehicle control systems of the future.

For the prolonged usage of PVDF sensors inside the tires, their thermal limitation issue needs to be addressed. Different coating materials might provide better thermal insulation and the sensors can still be operational at temperatures above 90C for automotive applications.

Signal degradation of PVDF sensors after extended usage should also be thoroughly analyzed. This might lead to making slight variations to the manufacturing process of the sensor itself.

# Appendix A

## PVDF Data Sheet

### LDT Series Elements with Lead Attachment and Lamination

The 'L' in LDT stands for 'laminated' sensor. Typically, a 0.005" (125µm) polyester layer is laminated to a 28 µm or 52µm piezo film element. When used in a 'bending' mode, laminated film elements develop much higher voltage output when flexed than a non-laminated DT elements series. The neutral axis is in the laminate instead of in the film so the film is strained more when flexed.

The capacitance is proportional to the area and inversely proportional to the thickness of the element.

Piezo film sensors LDT elements are available in a variety of lead attachment options. For significantly increased sensitivity, the LDTM-028K (M-Mass) combines an LDT0-028K form factor with the addition of a 0.72 gram round mass. The LDT1, 2 and 4 have 12" of 26 gauge twisted pair wire.

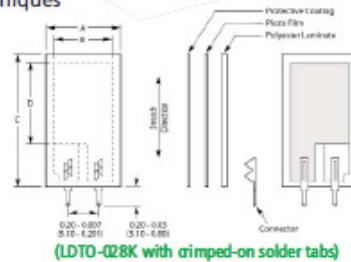
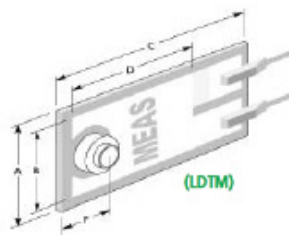
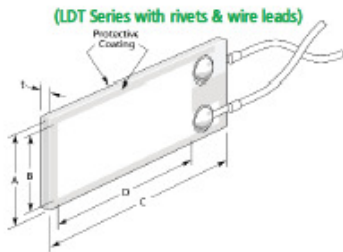
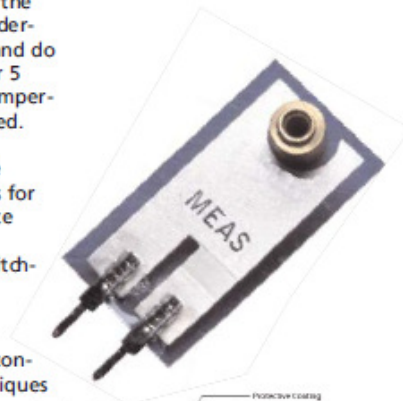
The LDT0-028K and LDTM-028K with solder tabs can be soldered directly to a PCB with

a reasonable level of care. Piezo film cannot withstand high temperatures (>80°C), and therefore soldering of the pins to a PCB must be done quickly. A heatsink clamped to the interface area between the film and the crimps will take the heat away from the film. Pre-tin the PCB and then quickly solder the sensor to the board. Do not allow the soldering iron to touch the film, and do not use a dwell time of over 5 seconds on the pins. Low temperature solders can also be used.

Applications for this include beam-type vibration sensors for vehide alarms and solid state switches for counters and momentary closure type switches.

For tightly tolerance sensitivity requirements, please consult MEAS Sensors for techniques

used to control variations of boundary conditions in production.



#### DIMENSIONS in INCHES (mm)

Description	A Film	B Electrode	C Film	D Electrode	t (µm)	Cap (nF)	Part Number
LDT0-028K/L w/crimps	.520 (13)	.400 (10)	.980 (25)	.580 (14.70)	205	.500	1002794
LDT1-028K/L w/rivets	.640 (16)	.484 (12)	1.63 (41)	1.19 (30.17)	205	1.38	1-1002910-0
LDT2-028K/L w/rivets	.640 (16)	.484 (12)	2.86 (72)	2.42(61.47)	205	2.78	1-1003745-0
LDT4-028K/L w/rivets	.860 (21)	.740 (18)	6.72 (170)	6.13 (155.70)	205	11.0	1-1002405-0
LDTM-028K/L w/crimps	.520 (13)	.400 (10)	.980 (25)	.580 (14.70)	205	.420	1005447-1

Effective: August 1<sup>st</sup>, 2008

Please contact the factory for pricing and custom part quotations.  
800.745.8008



# Appendix B

## Electronics Data Sheets

### ADC:



**LTC1857/LTC1858/LTC1859**  
8-Channel, 12-/14-/16-Bit,  
100ksps SoftSpan A/D  
Converters with Shutdown

#### FEATURES

- Sample Rate: 100ksps
- 8-Channel Multiplexer with  $\pm 25V$  Protection
- Single 5V Supply
- Software-Programmable Input Ranges:  
0V to 5V, 0V to 10V,  $\pm 5V$  or  $\pm 10V$   
Single Ended or Differential
- $\pm 3LSB$  INL for the LTC1859,  $\pm 1.5LSB$  INL for the LTC1858,  $\pm 1LSB$  INL for the LTC1857
- Power Dissipation: 40mW (Typ)
- SPI/MICROWIRE™ Compatible Serial I/O
- Power Shutdown: Nap and Sleep
- Signal-to-Noise Ratio: 87dB (Typ) for the LTC1859
- Operates with Internal or External Reference
- Internal Synchronized Clock
- 28-Pin SSOP Package

#### APPLICATIONS

- Industrial Process Control
- Multiplexed Data Acquisition Systems
- High Speed Data Acquisition for PCs
- Digital Signal Processing

#### DESCRIPTION

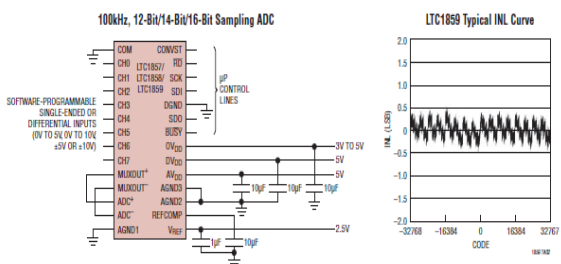
The LTC<sup>®</sup>1857/LTC1858/LTC1859 are 8-channel, low power, 12-/14-/16-bit, 100ksps, analog-to-digital converters (ADCs). These SoftSpan™ ADCs can be software-programmed for 0V to 5V, 0V to 10V,  $\pm 5V$  or  $\pm 10V$  input spans and operate from a single 5V supply. The 8-channel multiplexer can be programmed for single-ended inputs or pairs of differential inputs or combinations of both. In addition, all channels are fault protected to  $\pm 25V$ . A fault condition on any channel will not affect the conversion result of the selected channel.

An onboard high performance sample-and-hold and precision reference minimize external components. The low 40mW power dissipation is made even more attractive with two user selectable power shutdown modes. DC specifications include  $\pm 3LSB$  INL for the LTC1859,  $\pm 1.5LSB$  INL for the LTC1858 and  $\pm 1LSB$  for the LTC1857.

The internal clock is trimmed for 5µs maximum conversion time and the sampling rate is guaranteed at 100ksps. A separate convert start input and data ready signal (BUSY) ease connections to FIFOs, DSPs and microprocessors.

L<sup>™</sup>, LTC and LTM are registered trademarks of Linear Technology Corporation. SoftSpan is a trademark of Linear Technology Corporation. All other trademarks are the property of their respective owners.

#### TYPICAL APPLICATION



[www.linear.com](http://www.linear.com)

### Opamp:



**OPA277**  
**OPA2277**  
**OPA4277**

SBO3079A – MARCH 1999 – REVISED APRIL 2005

## High Precision OPERATIONAL AMPLIFIERS

#### FEATURES

- ULTRA LOW OFFSET VOLTAGE: 10µV
- ULTRA LOW DRIFT:  $\pm 0.1\mu V/^\circ C$
- HIGH OPEN-LOOP GAIN: 134dB
- HIGH COMMON-MODE REJECTION: 140dB
- HIGH POWER SUPPLY REJECTION: 130dB
- LOW BIAS CURRENT: 1nA max
- WIDE SUPPLY RANGE:  $\pm 2V$  to  $\pm 18V$
- LOW QUIESCENT CURRENT: 800µA/amplifier
- SINGLE, DUAL, AND QUAD VERSIONS
- REPLACES OP-07, OP-77, OP-177

#### DESCRIPTION

The OPA277 series precision op amps replace the industry standard OP-177. They offer improved noise, wider output voltage swing, and are twice as fast with half the quiescent current. Features include ultra low offset voltage and drift, low bias current, high common-mode rejection, and high power supply rejection. Single, dual, and quad versions have identical specifications for maximum design flexibility.

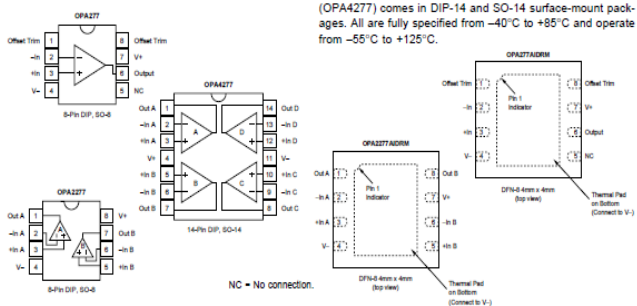
OPA277 series op amps operate from  $\pm 2V$  to  $\pm 18V$  supplies with excellent performance. Unlike most op amps which are specified at only one supply voltage, the OPA277 series is specified for real-world applications; a single limit applies over the  $\pm 5V$  to  $\pm 15V$  supply range. High performance is maintained as the amplifiers swing to their specified limits. Because the initial offset voltage ( $\pm 20\mu V$  max) is so low, user adjustment is usually not required. However, the single version (OPA277) provides external trim pins for special applications.

OPA277 op amps are easy to use and free from phase inversion and overload problems found in some other op amps. They are stable in unity gain and provide excellent dynamic behavior over a wide range of load conditions. Dual and quad versions feature completely independent circuitry for lowest crosstalk and freedom from interaction, even when overdriven or overloaded.

Single (OPA277) and dual (OPA2277) versions are available in DIP-8, SO-8, and DFN-8 (4mm x 4mm) packages. The quad (OPA4277) comes in DIP-14 and SO-14 surface-mount packages. All are fully specified from  $-40^\circ C$  to  $+85^\circ C$  and operate from  $-55^\circ C$  to  $+125^\circ C$ .

#### APPLICATIONS

- TRANSDUCER AMPLIFIER
- BRIDGE AMPLIFIER
- TEMPERATURE MEASUREMENTS
- STRAIN GAGE AMPLIFIER
- PRECISION INTEGRATOR
- BATTERY POWERED INSTRUMENTS
- TEST EQUIPMENT



**⚠** Please be aware that an important notice concerning availability, standard warranty, and use in critical applications of Texas Instruments semiconductor products and disclaimers thereto appears at the end of this data sheet. All trademarks are the property of their respective owners.

PRODUCTION DATA Information is current as of publication date. Products conform to specifications per the terms of Texas Instruments standard warranty. Production processing does not necessarily include testing of all parameters.

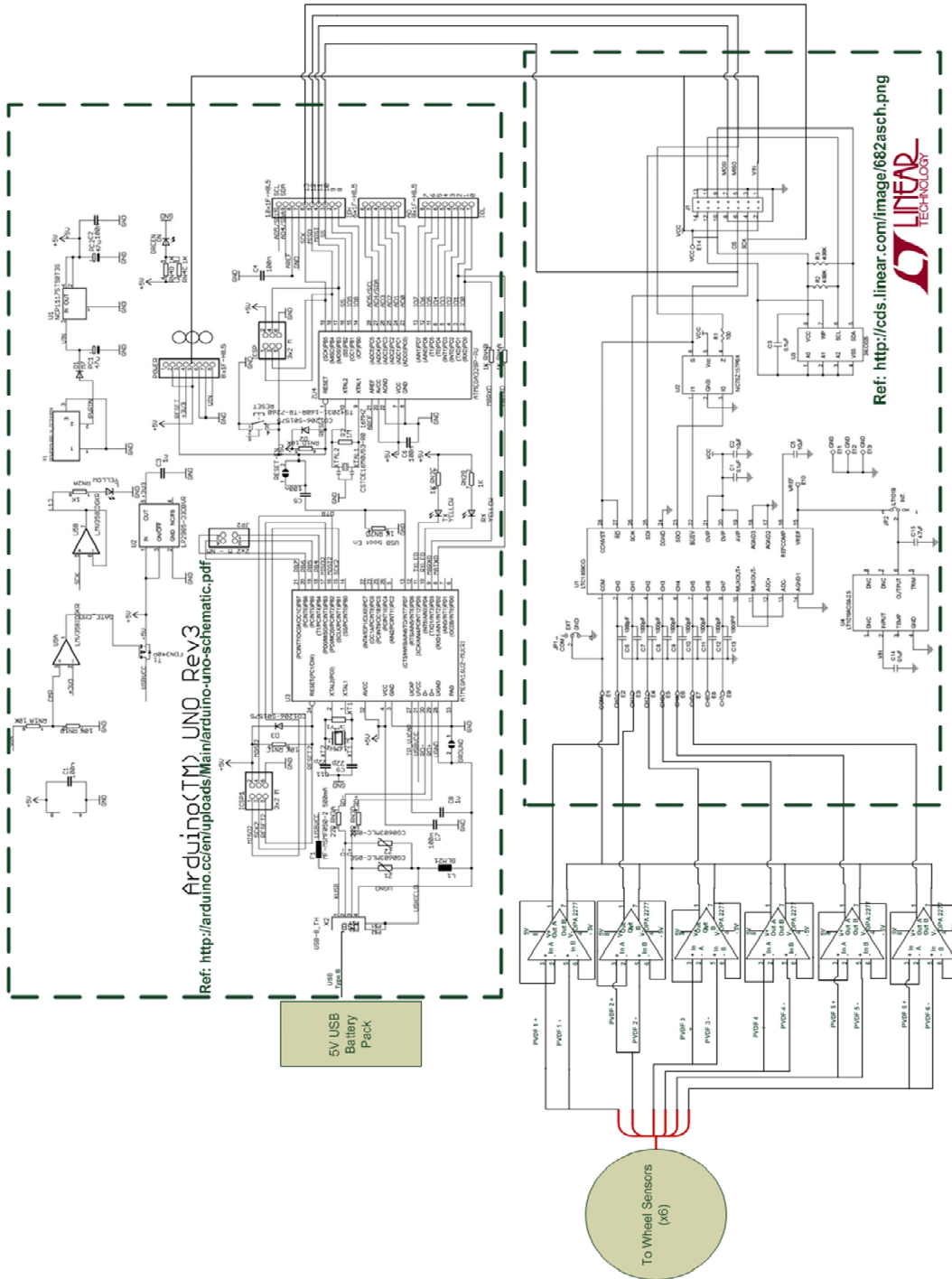


Copyright © 1999-2005, Texas Instruments Incorporated

[www.ti.com](http://www.ti.com)

# Appendix C

## Arduino DAQ Schematics



## Bibliography

- [1] D. Ammon, “Vehicle Dynamics Analysis Tasks And Related Tyre Simulation Challenges”, *Vehicle System Dynamics*, vol. 43, no. sup1, pp. 30–47, Jan. 2005.
- [2] R. M. Brach, N. Dame, B. Engineering, and R. M. Brach, “Tire Models for Vehicle Dynamic Simulation and Accident Reconstruction”, *SAE International* vol. 01-0102, 2009.
- [3] F. Cheli, F. Braghin, M. Brusarosco, F. Mancosu, and E. Sabbioni, “Design And Testing Of An Innovative Measurement Device For Tyre–Road Contact Forces”, *Mechanical Systems and Signal Processing*, vol. 25, no. 6, pp. 1956–1972, Aug. 2011.
- [4] G. Erdogan, L. Alexander, and R. Rajamani, “Estimation of Tire-Road Friction Coefficient Using a Novel Wireless Piezoelectric Tire Sensor”, *IEEE Sensors Journal*, vol. 11, no. 2, pp. 267–279, 2011.
- [5] Y. Zhang, S. Member, J. Yi, S. Member, and T. Liu, “Embedded Flexible Force Sensor for In-Situ Tire – Road Interaction Measurements”, *IEEE Sensors Journal*, vol. 13, no. 5, pp. 1756–1765, 2013.
- [6] J. Dakhlallah, S. Glaser, S. Mammam, and Y. Sebsadji, “Tire-Road Forces Estimation Using Extended Kalman Filter and Sideslip Angle Evaluation”, *American Control Conference*, pp. 4597–4602, 2008.
- [7] D. Deliverable, D. Ag, and D. C. Ag, “Intelligent Tyre Systems – State of the Art and Potential Technologies”, *Project Report, European Community, IST-2001-34372*, 2003.
- [8] J. Yi and S. Member, “A Piezo-Sensor-Based Smart Tire System for Mobile Robots and Vehicles”, *IEEE/ASME Transactions on Mechatronics*, vol. 13, no. 1, pp. 95–103, 2008.
- [9] J. W. Sohn, J. Jeon, and S.-B. Choi, “An Investigation on Dynamic Signals of MFC and PVDF Sensors: Experimental Work”, *Advances in Mechanical Engineering*, vol. 2013, pp. 1–9, 2013.
- [10] R. Matsuzaki, T. Keating, A. Todoroki, and N. Hiraoka, “Rubber-Based Strain Sensor Fabricated Using Photolithography For Intelligent Tires”, *Sensors Actuators*, vol. 148, no. 1, pp. 1–9, Nov. 2008.
- [11] R. Matsuzaki and A. Todoroki, “Wireless Flexible Capacitive Sensor Based On Ultra-Flexible Epoxy Resin For Strain Measurement Of Automobile Tires”, *Sensors Actuators*, vol. 140, no. 1, pp. 32–42, Oct. 2007.
- [12] M. Sergio, N. Manaresi, M. Tartagni, R. Canegallo, and R. Guerrieri, “On A Road Tire Deformation Measurement System Using A Capacitive–Resistive Sensor”, *Smart Materials and Structures*, vol. 15, no. 6, pp. 1700–1706, Dec. 2006.

- [13] R. Matsuzaki and A. Todoroki, “Wireless Flexible Capacitive Sensor Based On Ultra-Flexible Epoxy Resin For Strain Measurement Of Automobile Tires”, *Sensors Actuators*, vol. 140, no. 1, pp. 32–42, Oct. 2007.
- [14] A. Todoroki, S. Miyatani, and Y. Shimamura, “Wireless Strain Monitoring Using Electrical Capacitance Change Of Tire: Part I—With Oscillating Circuit”, *Smart Materials and Structures*, vol. 12, no. 3, pp. 403–409, Jun. 2003.
- [15] R. Matsuzaki and A. Todoroki, “Wireless Monitoring of Automobile Tires for Intelligent Tires”, *Sensors*, vol. 8, no. 12, pp. 8123–8138, Dec. 2008.
- [16] R. Matsuzaki and A. Todoroki, “Wireless Strain Monitoring Of Tires Using Electrical Capacitance Changes With An Oscillating Circuit”, *Sensors Actuators*, vol. 119, no. 2, pp. 323–331, Apr. 2005.
- [17] R. Matsuzaki and A. Todoroki, “Passive Wireless Strain Monitoring Of Actual Tire Using Capacitance–Resistance Change And Multiple Spectral Features”, *Sensors Actuators*, vol. 126, no. 2, pp. 277–286, Feb. 2006.
- [18] A. Pohl, R. Steindl, and L. Reindl, “The ‘Intelligent Tire’ Utilizing Passive Saw Sensors Measurement Of Tire Friction”, *IEEE Transactions on Instrumentation and Measurement*, vol. 48, no. 6, pp. 1041–1046, 1999.
- [19] O. Yilmazoglu, M. Brandt, J. Sigmund, E. Genc, and H. L. Hartnagel, “Integrated InAs / GaSb 3D Magnetic Sensors For The Intelligent Tire”, *Sensors and Actuators*, vol. 94, pp. 59–63, 2001.
- [20] F. Braghin, M. Brusarosco, F. Cheli, a. Cigada, S. Manzoni, and F. Mancosu, “Measurement Of Contact Forces And Patch Features By Means Of Accelerometers Fixed Inside The Tire To Improve Future Car Active Control”, *Vehicle System Dynamics*, vol. 44, no. sup1, pp. 3–13, Jan. 2006.
- [21] M. Kreuzer, “Strain Measurement with Fiber Bragg Grating Sensors”, Product Whitepaper, HBM, Darmstadt, Germany, 1969.
- [22] K. Shimo, “Dynamic Shape And Strain Measurements Of Rotating Tire Using A Sampling Moiré Method”, *Optical Engineering*, vol. 50, no. 10, pp. 1 - 8, Oct. 2011.
- [23] R. W. Green, “A Non-contact Method for Sensing Tire Contact Patch Deformation Using a Monocular Vision System and Speckled Image Tracking”, Masters Thesis, Auburn University, 2011.
- [24] G. J. Nga, “Study on Electromagnetic Wave Propagation Characteristics in Rotating Environments and Its Application in Tire Pressure Monitoring”, *IEEE Transactions on Instrumentation and Measurement*, vol. 61, no. 6, pp. 1765–1777, Jun. 2012.

- [25] L. Tang, K.-C. Wang, and Y. Huang, "Study of Speed-Dependent Packet Error Rate for Wireless Sensor on Rotating Mechanical Structures", *IEEE Transactions on Industrial Informatics*, vol. 9, no. 1, pp. 72–80, Feb. 2013.
- [26] J. Si, S. a Colgate, H. Li, J. Martinic, and D. Westpfahl, "Data Acquisition In A High-Speed Rotating Frame For New Mexico Institute Of Mining And Technology Liquid Sodium  $\alpha\omega$  Dynamo Experiment", *Review of Scientific Instruments*, vol. 84, no. 10, pp. 1-11, Oct. 2013.
- [27] J. Sousa, a. J. N. Batista, a. Combo, R. Pereira, M. Correia, N. Cruz, P. Carvalho, C. Correia, and C. a. F. Varandas, "PCI Data Acquisition And Signal Processing Hardware Modules For Long Pulse Operation", *Review of Scientific Instruments*, vol. 75, no. 10, pp. 4271–4273, Oct. 2004.
- [28] P. Pillard, F. X. Ferrand, and E. Viguier, "3D Accelerometric Gait Analysis In Dogs Using Smartphone", *Computer Methods in Biomechanics and Biomedical Engineering*, vol. 16 Suppl 1, pp. 136–138, Jan. 2013.
- [29] F. J. Ferrero Martín, M. Valledor Llopis, J. C. Campo Rodríguez, J. R. Blanco González, and J. Menéndez Blanco, "Low-Cost Open-Source Multifunction Data Acquisition System For Accurate Measurements", *Measurement*, vol. 55, pp. 265–271, Sep. 2014.
- [30] H. R. Barnard, M. C. Findley, and J. Csavina, "PARduino: A Simple And Inexpensive Device For Logging Photosynthetically Active Radiation", *Technical Note, Tree Physiology*, vol. 34, no. 6, pp. 640–645, Jun. 2014.
- [31] T. T. Toh, P. D. Mitcheson, A. S. Holmes, and E. M. Yeatman, "A Continuously Rotating Energy Harvester With Maximum Power Point Tracking", *Journal of Micromechanics and Microengineering*, vol. 18, no. 10, pp. 1-7, Oct. 2008.
- [32] K. Il Lee, B. J. Lim, S. H. Kim, and Y. Hong, "Energy Harvesting By Rotation Of Wheel For Tire Monitoring System", *IEEE Sensors*, pp. 1–4, Oct. 2012.
- [33] S. J. Round, J. Tola, "An Energy Harvester For Rotating Environments", *Transducers*, pp. 689–692, June 2013.
- [34] N. G. Elvin, A. Elvin, M. Spector, "A Self-Powered Mechanical Strain Energy Sensor", *Smart Materials and Structures*, vol. 10, no. 2, pp. 293–299, Apr. 2001.
- [35] Pacejka, H., Bakker, E., Nyborg, L., 1987, "Tyre Modelling for Use in Vehicle Dynamic Studies", SAE International, USA
- [36] Karray, F., Silva, C., 2004, "Soft Computing and Intelligent Systems Design", Pearson Addison Wesley, England
- [37] Rackety Raphael: IP Rating Chart, <http://www.racketyraphael.com/lg-g3/ip-rating-chart/>, Retrieved: September 5, 2014

- [38] Bastiaan, J. M., 2013, "Design of a Smart Tire Sensor System", Ph.D. Research Proposal, Comprehensive Examination Date: February 15, 2013, University of Waterloo, Waterloo, ON
- [39] NASA's Space Shuttle Program With MICHELIN® Aircraft Tires, <http://www.airmichelin.com/generalcontent.aspx?id=149>, Retrieved: June 4, 2014
- [40] Wheel Transducers | Michigan Scientific Corporation [http://www.michsci.com/Products/transducers/wheel\\_transducers.htm](http://www.michsci.com/Products/transducers/wheel_transducers.htm), Retrieved: June, 2014
- [41] Young's Modulus - Wikipedia, the free encyclopedia [http://en.wikipedia.org/wiki/Young's\\_modulus](http://en.wikipedia.org/wiki/Young's_modulus), Retrieved: June 4, 2014
- [42] MTS | Flat-Trac <http://www.mts.com/en/products/producttype/test-systems/simulation-systems/tire/flat-trac/index.htm>, Retrieved: June 4, 2014
- [43] Strain Gauges : Electrical Instrumentation Signals - Electronics Textbook [http://www.allaboutcircuits.com/vol\\_1/chpt\\_9/7.html](http://www.allaboutcircuits.com/vol_1/chpt_9/7.html), Retrieved: June 4, 2014
- [44] Why Temperature?, <http://www.valortpms.com/whytemperature.php>, Retrieved: June 4, 2014
- [45] Liquidware : Lithium Backpack, <http://www.liquidware.com/shop/show/MBP/Lithium+Backpack>, Retrieved: July 12, 2014